# Targeting the PI3K Pathway in Esophago-Gastric Cancer

Philip Pisano

Faculty of Medicine

Division of Experimental Surgery

McGill University, Montreal, Canada

Supervisors: Dr. Lorenzo Edwin Ferri MD, PhD and Dr. Veena Sangwan, PhD


April 2020

A thesis submitted to McGill University in partial fulfillment of the requirements of the degree

of Master of Science in Experimental Surgery

# TABLE OF CONTENTS

## ABSTRACT

Gastric and esophageal cancers represent the 3rd and 6th deadliest cancers worldwide with a five-year survival of 25% and 15% respectively. Regardless of their high mortality rates, research has remained underfunded which has stalled the advancement of novel therapies. The current standard-of-care for patients diagnosed with esophago-gastric cancer (EGC) is the surgical removal of the tumor accompanied by perioperative Docetaxel-based triplet chemotherapy (DCF: Docetaxel, Cisplatin, 5-FU). Although this is the most effective regimen for treating EGC to date, only 60% of patients initially respond to treatment, of which 50% develop resistance. Targeted therapies guided by molecular testing have largely been unsuccessful, with the exception of Trastuzumab in HER2 amplified tumors and angiogenesis inhibitors for second-line treatment. AT-rich interaction domain 1A (ARID1A) is altered in about 30% of EGCs. However, ARID1A mutations frequently co-occur with mutations in the PI3K/AKT/mTOR pathway. We aimed to investigate ARID1A as a potential biomarker for PI3K and MAPK pathway targeting agents.

33 patient-derived xenografts (PDXs) were sent for next-generation sequencing to analyze copy number variations (CNVs) and single nucleotide polymorphisms (SNPs). Western blot analysis from PDX protein lysates were used to compare protein expression levels with sequencing data. Organoids derived from PDXs were used to perform *in-vitro* high-throughput drug screens using PI3K and MAPK pathway targeting inhibitors.

Our cohort of patients displayed a high frequency of ARID1A alterations (45%), which was found to frequently co-occur with activating mutations in EGFR (67%), BRAF (60%), KRAS (40%), PIK3CA (40%), PIK3CG (60%), RICTOR (40%) and RPTOR (33%). Western blot analysis confirmed lack of ARID1A expression in ARID1A-mutant PDXs, while also

highlighting that 80% of those PDXs displayed activation of ERK. High-throughput drug screening on two PDX-derived organoid lines showed greatest sensitivity to the MEK inhibitor Trametinib and ERK inhibitor Ulixertinib. However, further screening with 13 other organoid lines showed no concordance between ARID1A loss and drug sensitivity. Similarly, additional MEK and ERK inhibitors tested showed reduced sensitivity, suggesting Trametinib and Ulixertinib were acting in a non-specific manner. A potential alternative may be the dual PIK3CA/mTOR inhibitor Gedatolisib, which showed greatest sensitivity in organoid lines with ARID1A loss and mutations in PI3K and RICTOR. These studies have shown the promise of using ARID1A as a biomarker for PI3K pathway targeting, although further investigation is required.

## RÉSUMÉ

Les cancers gastriques et œsophagiens sont les 3e et 6e cancers les plus meurtriers dans le monde et leur taux de survie à cinq ans est estimé à 25% et 15%, respectivement. En dépit de leurs taux de mortalité élevés, la recherche spécifique à ce type de cancer demeure sous-financée, ce qui freine le développement de nouvelles thérapies. Pour les patients diagnostiqués d'un cancer œsophago-gastrique (EGC), la norme de soins actuelle est l'ablation chirurgicale de la tumeur accompagnée d'une triple chimiothérapie périopératoire à base de Docétaxel (DCF : Docetaxel, Cisplatin, 5-FU). Malgré le fait que ce soit le traitement de l'EGC le plus efficace à ce jour, seulement 60% des patients y répondent initialement et plus de 50% d'entre eux développeront de la résistance médicamenteuse. Plusieurs tests de thérapies moléculaires ciblées ont largement échoué, à l'exception de celui impliquant l'utilisation du Trastuzumab, couplé à des inhibiteurs d'angiogénèse en deuxième ligne, pour les tumeurs dans lesquelles HER2 est amplifié. ARID1A (domaine d'interaction riche en AT 1A) est muté dans environ 30% des EGC. En outre, les mutations dans ARID1A sont souvent co-exprimées avec des mutations dans la voie de signalisation PI3K/AKT/mTOR. Nous avons donc voulu étudier le rôle d'ARID1A en tant que biomarqueur lors de l'utilisation d'agents de chimiothérapie spécifiques aux voies de signalisation PI3K et MAPK.

33 tumeurs primaires de patients EGC ont été implantées par voie sous-cutanée dans des souris (PDX) et se sont développées jusqu'à 300 $mm^3$. Elles ont été prélevées et le séquençage de nouvelle génération a été fait afin d'analyser les variations du nombre de copies (CNV) et les polymorphismes mononucléotidiques (SNP) dans ces tumeurs. Une analyse par immunobavardage à partir de lysats de protéines des PDX a été faite afin de comparer les niveaux d'expression des protéines avec les données de séquençage. Les lignées cellulaires

d'organoïdes dérivés des PDX ont été utilisés pour effectuer des criblages de médicaments à haut débit en utilisant une multitude d'inhibiteurs ciblant les voies PI3K et MAPK.

Dans notre cohorte de patients, nous avons trouvé une fréquence élevée de mutations dans ARID1A (45%), altérations fréquemment co-exprimées avec des mutations activatrices d'EGFR (67%), de BRAF (60%), de KRAS (40%), de PIK3CA (40%), de PIK3CG (60%), de RICTOR (40%) et de RPTOR (33%). L'analyse par immunobuvardage a confirmé l'absence de la protéine ARID1A dans les PDX exprimant des mutations dans le gène ainsi qu'une activation de ERK1/2 dans 80% de ces échantillons. Le criblage de médicaments à haut débit sur deux lignées cellulaires d'organoïdes dérivés de PDX a montré une plus grande sensibilité à l'inhibiteur MEK Trametinib et à l'inhibiteur ERK Ulixertinib. Cependant, un dépistage supplémentaire avec 13 autres lignées d'organoïdes n'a montré aucune concordance entre la perte d'ARID1A et la sensibilité à ces drogues. Finalement, d'autres inhibiteurs de MEK et de ERK testés ont aussi montré une sensibilité réduite, suggérant alors que le Trametinib et l'Ulixertinib agiraient probablement de manière non-spécifique. Une alternative potentielle pourrait être le double inhibiteur PIK3CA/mTOR Gedatolisib, qui a montré une plus grande sensibilité dans les lignées d'organoïdes présentant une perte d'ARID1A et des mutations dans PI3K et RICTOR. Bien que des recherches supplémentaires soient nécessaires, ces travaux nous éclairent sur le potentiel prometteur d'ARID1A afin de devenir un biomarqueur pour le ciblage de la voie PI3K.

**ACKNOWLEDGEMENTS**

I would like to thank my supervisors, Dr. Lorenzo Ferri and Dr. Veena Sangwan for giving me the opportunity to conduct such meaningful research in their lab. Being able to work with two incredible minds with such varied backgrounds allowed me to gain so much insight. From Dr. Ferris clinical background to Dr. Sangwans basic science background I was able to apply my basic science skills in a way that become meaningful from a clinical perspective which I feel made my masters even better. I want to thank you for your dedication and continuously helping me whenever I would hit a roadblock with my project by giving me new insights into how I can manage to proceed further. I would especially like to thank Dr. Sangwan for always being there for me, no matter the time of day to answer any questions I had. The dedication my PIs possess for this research has both astounded and inspired me. I would also like to thank my committee, including Dr. Fackson Mwale and Dr. Simon Rousseau for their advice and inspiration throughout my degree. I would like to give a special thank you to Julie Berube for her incredible help in the lab, from taking care of orders, teaching me basic techniques, giving overall guidance and as simply as making me smile in the lab. I'd also like to give a special thank you to my other lab mates at the MGH, Sabrina, Jeff and Olivia, who created such a great environment to work in and made going into the lab fun, even on the worst of days. I would also like to thank my lab mates at the Glen, who although I didn't see quite as often, always welcomed me with support when I would come to work or practice gavage at the Glen. Another special thank you to France for helping me learn mouse handling and techniques, and your amazing patience throughout the whole ordeal. I am also very grateful for Betty for taking care of all administrating and access issues throughout my degree.

I'd also like to give one of my sincerest acknowledgments to Dr. Hellen Kuasne, who I learned almost everything I know from. You taught me just about everything in terms of organoid culture and really helped steer my project in the right direction. I am so grateful I got to work with you as you are one of the nicest people I have ever met and would continuously be there for me when I needed help. I would also like to thank Dr. Morag Park for letting me work in your lab for well over a year. I also want to give a special thank you to the entire Park lab, who always greeted me with a smile and made me feel so welcome in the lab. While working there I truly felt like an adopted member of your lab.

I'd also like to acknowledge my friends, Amanda, Arashdeep and Lorie who have supported me on my best and worst days, I don't know what I would do without you. My family deserves a special acknowledgement as well as they have supported me from the day I was born and motivated me to continue and always strive for whatever I wanted. Thank you to everyone, as this would not have been possible without all your contributions, academically or not.

## PREFACE & AUHOR CONTRIBUTIONS

This thesis was written in accordance with the guidelines outlined by the Faculty of Graduate and Postdoctoral Studies of McGill University. All parts of this thesis were written exclusively by the author, Philip Pisano. The author did the experimental design, laboratory work and data analysis under the supervision and guidance of Dr. Lorenzo Ferri and Dr. Veena Sangwan. Sequencing data report was performed by the author, although the analysis was performed by Dr. Hellen Kuasne from Dr. Morag Parks lab. Furthermore, 7 PDX-derived organoid lines tested for Trametinib and Gedatolisib response were performed by Dr. Hellen Kuasne and were reported in this thesis with her approval (lines: GP201425, GP201452, GP201571, GP201585, GP2015105, GP2015118, G1655829).

## LIST OF ABBREVIATIONS

| | |
|---|---|
| 4E-BP1 | Eukaryotic initiation factor 4E |
| 5-FU | 5-Fluorouracil |
| AKT | RAC-alpha serine/threonine-protein kinase |
| APC | Adenomatous polyposis coli |
| ARID1A | AT-rich interactive domain 1A |
| ANXA1 | Annexin A1 |
| ATR | Ataxia telangiectasia and Rad3 |
| BAX | Bcl-2-associated X |
| BRAF | Raf murine sarcoma viral oncogene homolog B |
| BSA | Bovine serum albumin |
| CAS9 | CRISPR-associated protein 9 |
| CCDN1 | Cyclin D1 |
| CCL | Cancer cell line |
| CDH1 | Cadherin 1 |
| CDK2NA | Cyclin-dependent kinase inhibitor 2A |
| CIN | Chromosomal instability |
| CNV | Copy number variation |
| CTLA4 | Cytotoxic T-lymphocyte antigen 4 |
| CRISPR | Clustered Regulatory Interspaced Short Palindromic Repeats |
| DCF | Docetaxel, Cisplatin and 5-FU |
| DMEM | Dulbecco's modified eagle medium |
| DMSO | Dimethylsulfoxide |

| | |
|---|---|
| EA | Esophageal adenocarcinoma |
| EBV | Epstein-Barr virus |
| ECL | Enhanced chemiluminescence |
| ECX | Epirubicin, Cisplatin and Capecitabine |
| EDTA | Ethylenediaminetetraacetic acid |
| EGA | Esophago-Gastric adenocarcinoma |
| EGC | Esophago-Gastric cancer |
| EGF | Epidermal growth factor |
| EGFR | Epidermal growth factor receptor |
| ERBB | Erythroblastic oncogene B |
| ERK | Extracellular signal-regulated kinase |
| ESCC | Esophageal squamous cell carcinoma |
| EZH2 | Enhancer of zeste homolog 2 |
| FBS | Fetal Bovine Serum |
| FDA | Food and Drug Administration |
| FGF | Fibroblast growth factor |
| FGFR | Fibroblast growth factor receptor |
| FISH | Fluorescent insitu hybridization |
| GEJ | Gastroesophageal junction |
| GERD | Gastroesophageal reflux disease |
| GPCR | G protein coupled receptor |
| GS | Genomically stable |
| GTP | Guanosine triphosphate |

| | |
|---|---|
| HDAC6 | Histone deacetylase 6 |
| HER2 | Human epidermal growth factor receptor 2 |
| HGF | Hepatocyte growth factor |
| HRP | Horseradish Peroxidase |
| HSP90 | Heat shock protein 90 |
| IHC | Immunohistochemical |
| KDM6A | Lysine demethylase 6A |
| KRAS | Kristen rat sarcoma 2 viral oncogene homolog |
| LGR5 | Leucine-rich repeat-containing G-protein coupled receptor 5 |
| MAPK | Mitogen-activated protein kinase |
| MDM2 | Mouse double minute 2 homolog |
| MEK | Mitogen-activated protein kinase kinase |
| MET | MNNG-HOS transforming gene |
| MGH | Montreal General Hospital |
| MLH1 | MutL homolog 1 |
| MSI | Microsatellite instability |
| MTOR | Mammalian target of rapamycin |
| MUHC | McGill University Health Center |
| NGS | Next generation sequencing |
| NSCLC | Non-small cell lung cancer |
| NSG | Nod scid gamma |
| OCCC | Ovarian clear cell carcinoma |
| OS | Overall survival |

| | |
|---|---|
| PAGE | Polyacrylamide gel electrophoresis |
| PBS | Phosphate-buffered saline |
| PD-1 | Programmed cell death protein 1 |
| PD-L1 | Programmed cell death protein ligand 1 |
| PDK | Phosphoinositide-dependent kinase |
| PDO | Patient-derived organoid |
| PDX | Patient-derived xenograft |
| PFA | Paraformaldehyde |
| PFS | Progression free survival |
| PI3K | Phosphoinositide 3-kinase |
| PIK3CA | Phosphatidylinositol-4,5-biphosphate 3-Kianse Catalytic Subunit Alpha |
| PIK3IP1 | Phosphoinosiide-3-kinase interacting protein 1 |
| PMSF | Phenylmethylsulfonyl fluoride |
| PTEN | Phosphatase and tensin homolog |
| PVDF | Polyvinylidene fluoride |
| RHOA | Ras homolog gene family, member A |
| RICTOR | Rapamycin-insensitive companion of mammalian target of rapamycin |
| RIPA | Radioimmunoprecipitation assay |
| RPTOR | Regulatory-associated protein of mammalian target of rapamycin |
| RTK | Receptor tyrosine kinase |
| S6K1 | Ribosomal S6 protein |
| SDS | Sodium dodecyl sulfate |
| SHP2 | Src homology 2-containing phosphotyrosine phosphatase |

| | |
|---|---|
| SMAD4 | Mothers against decapentaplegic homolog 4 |
| SMARCA | SWI/SNF-related, matrix associated, actin depend regulator chromatin group A |
| SNP | Single nucleotide polymorphism |
| SOS | Son of sevenless homolog |
| SOX2 | Sex determining region Y-box 2 |
| STAT3 | Signal Transducer and activator of transcription 3 |
| STK11 | Serine/threonine kinase 11 |
| SWI/SNF | SWItch/Sucrose non-fermenting |
| TBS | Tris-buffered saline |
| TCGA | The Cancer Genome Atlas |
| TKI | Tyrosine kinase inhibitor |
| TME | Tumor microenvironment |
| TP53 | Tumor protein 53 |
| TP63 | Tumor protein 63 |
| TSC1 | Tuberous sclerosis 1 |
| UTR | Untranslated region |
| VEGF | Vascular endothelial growth factor |
| VEGFR | Vascular endothelial growth factor receptor |
| WT | Wild type |

## LIST OF FIGURES & TABLES

# CHAPTER 1: REVIEW OF THE LITERATURE

## 1.1 Gastric and Esophageal Cancer

### 1.1.1 Gastric and esophageal cancer: categories and trends

Gastric and esophageal cancers have offered a substantial clinical challenge accounting for 783,000 and 400,000 cancer-related deaths worldwide in 2018, representing the 3rd and 6th deadliest cancer types respectively[1-3]. In Canada, the five-year survival rate for patients diagnosed with gastric cancer is 25%, whereas that for esophageal cancer is only 15%[4]. These low five-year survival rates are attributed to the difficulty in diagnosing patients until later stage disease, where metastasis develops and prognosis becomes poor[5]. Although the incidence rates for gastric and esophageal cancer vary dramatically geographically, there has been an overall steady decline in incidence for these two diseases worldwide over the last few decades[2,5]. This is due to a number of factors including screening for early detection, dietary improvements, anti *H-pylori* therapies and improved chemotherapy regimens[5-7].

Gastric adenocarcinoma accounts for 90% of all gastric cancer cases and has seen a steady decline in incidence in the last few decades[8,9]. Historically, gastric cancer has been classified into two main histological subgroups based on the Lauren criteria: intestinal and diffuse. Intestinal gastric tumors are the most common with a frequency of 54% and are marked by extensive adhesive properties and tubular formations[10]. These tumors are commonly associated with environmental factors such as diet, lifestyle and *H-pylori* infection[11]. Diffuse gastric tumors have a relative frequency of 32% and are associated with shorter durations but poorer prognosis[10]. Diffuse tumor cells lack proper adhesive functions and exhibit stromal

infiltration, which often leads to peritoneal metastasis[11]. Diffuse gastric tumors are more common in younger and female patients and are more commonly caused by genetic factors[12]. Esophageal cancer is classified into two main subtypes: adenocarcinoma and squamous cell carcinoma. There are more annual reported cases of esophageal squamous cell carcinoma (ESCC) than esophageal adenocarcinoma (EA) worldwide[13].

Unlike gastric adenocarcinoma, the overall incidence rates for esophageal adenocarcinoma have shown a sharp increase in North America, making EA the predominant subtype in many developed countries[14]. This is in part due to the obesity epidemic, which increases the populations risk of developing gastroesophageal reflux disease (GERD), a condition which causes the spillage of stomach acid into the esophagus and promotes the development of a Barrett's esophagus, a common precursor for EA[15].

### 1.1.2 Treating Esophago-Gastric Cancer with Perioperative Chemotherapy

Comparable genetic profiles of adenocarcinomas of the proximal stomach, distal esophagus and gastro-esophageal junction (GEJ) have suggested that these adenocarcinomas be considered as one disease entity, esophago-gastric adenocarcinoma (EGA) and treated similarly[16]. Standard-of-care after diagnosis is currently limited to perioperative Docetaxel-based triplet therapy with the surgical removal of the tumor. Ferri et al. showed that treatment of resectable EGA with DCF (Docetaxel, Cisplatin and 5-Fluoruricil at doses of 75mg/m$^2$, 75mg/m$^2$ and 750mg/m$^2$ respectively), 3 weeks prior to and following surgery significantly improved patient outcome[17]. Others had previously shown that pairing surgical resection with perioperative chemotherapy regimens significantly improved patient survival compared to patients receiving surgery alone[18,19]. Van Hagen et al. studied the role of neoadjuvant chemoradiotherapy in the

treatment of patients with GEJ cancer and mixed-subtype esophageal cancers. They determined that administration of Carboplatin and Paclitaxel with radiotherapy of 41.4Gy for at least 4 weeks prior to surgery conferred greater survival benefit than surgery alone[20]. Stahl et al. investigated whether the addition of radiotherapy improved EGA patient outcome compared to standard chemotherapy regimens. They observed a benefit of including radiotherapy in neoadjuvant treatment, although this improvement was not significant[21]. Regardless of the 5-year survival benefit conferred with DCF chemotherapy regimens, only 60% of patients initially respond to treatment due to innate chemoresistance. Furthermore, of the patients who initially respond nearly half develop resistance to treatment and any residual disease leads to patient recurrence, highlighting the need for finding better therapeutic options[22].

### 1.1.3 Treating Esophago-Gastric Cancer with Immunotherapy

Immune checkpoint inhibitors targeting the Programmed cell death protein 1 or its ligand, PDL-1, have been studied more recently in patients with esophageal and gastric cancers. A phase III clinical trial (ATTRACTION-2) investigating the treatment of Nivolumab, a PD-L1 inhibitor, in advanced gastric cancer patients who had previously undergone chemotherapy, showed an increase in overall survival (OS) compared to placebo group (26.6% vs. 10.9% after 12 months)[23]. Nivolumab is now accepted as a third line of treatment strategy for EGC patients and ongoing clinical trials are determining its impact as a first line of treatment[24]. Similarly, a phase IB clinical trial (KEYNOTE-012) compared the treatment of Pembrolizumab immunotherapy with Paclitaxel chemotherapy as a second line of treatment for gastric and GEJ patients. Although there was no improvement in OS between the two groups, patients overexpressing PD-1 performed better with Pembrolizumab[25]. In a phase II clinical trial, Ipilimumab, a target of

cytotoxic T-lymphocyte antigen 4 (CTLA4) showed no clinical significance against standard chemotherapy[26]. Although there are many ongoing clinical trials looking at immunotherapy as first-line treatments, current outcomes are modest at best and show little clinical utility for immunotherapies.

### 1.1.4 Molecular Classification of Esophago-Gastric Cancer

Classically, gastric tumors are histologically classified as intestinal or diffuse types, although this has little clinical utility. After molecular evaluation, gastric tumors were found to exist as four distinct subtypes: Epstein-Barr virus (EBV; 9%), Microsatellite instability (MSI; 22%), Genomically stable (GS; 20%) and Chromosomal instability (CIN; 50%)[27]. EBV-positive tumors represent the smallest proportion and are marked by CDK2NA silencing, PD-L1 overexpression and ARID1A/PIK3CA mutations. MSI variant tumours are hypermutated and show hypermethylation, most notably of MLH1. GS variants are marked by a 'diffuse' histology, with mutations in adhesion molecules such as CDH1 and RhoA. The CIN variants represent half of all gastric tumors and exhibit an 'intestinal' histology, with TP53 mutations and hyperactivation of receptor tyrosine kinase's such as EGFR and ERBB2.

Similarly, comprehensive molecular analysis was done on esophageal tumors and established EAC and ESCC as separate disease entities with divergent patterns of mRNA expression, DNA methylation and cancer location[28]. ESCC tumors were localized to the upper esophagus and resembled the genetic profiles of head and neck squamous cell carcinomas. ESCC's exhibited gene amplifications of CCDN1, TP63 and SOX2 as well as gene deletions of ARID1A, SMARCA4 and KDM6A[29]. EACs were primarily localized in the distal esophagus and genetically resembled the CIN subtype for gastric adenocarcinomas, with RTK amplifications.

These molecular classifications for gastric and esophageal cancers are critical to better stratify patients based on genetic alterations and find more effective and personalized treatment options.

### 1.1.5 Molecular Heterogeneity as a Barrier for Targeted Therapeutics

Using genomic biomarkers to guide targeted therapies for EGC patients has yet to show significant clinical impact. One of the only genomic biomarkers used in the clinic is the Human epidermal growth factor receptor 2 (HER2), which is highly enriched in the CIN subtype[27]. HER2 is overexpressed in approximately 18% of gastric tumors, whereby these tumors are highly sensitive to anti-HER2 targeted therapies[30]. In a phase III clinical trial, treatment of advanced gastric and GEJ cancer with Trastuzumab, a monoclonal antibody directed against HER2, in combination with chemotherapy showed a moderate increase in OS (4.2 months) in 'HER2-positive' patients compared to chemotherapy alone[31]. Further anti-HER2 targeted therapies involving Lapatinib or Pertuzumab showed no significant clinical value compared to chemotherapy[32,33]. Trastuzumab is the first targeted therapy guided by molecular testing for gastric cancer. Many other targeted therapies, even guided by genomic biomarkers, showed limited efficacy in the clinic, including therapies directed against EGFR, FGFR2 and MET[32,34,35]. Delays in novel targeted therapies for EGC have been attributed to the baseline heterogeneity found between different patients (*inter*-tumor) and within different sites of a patient's tumor (*intra*-tumor)[36]. Whole-exome sequencing revealed a lack of concordance between the genomic profiles of a patients primary tumor and that at the metastatic site[36]. Similarly, genetic variability was also observed within the patient's primary tumor. The PANGEA cohort study investigated the value of targeted therapies and the discordance between the primary and metastatic tumor sites, as most treatments are assessed based on biopsies from primary tumor samples. Patients

biomarked at both the metastatic and primary tumor sites showed reduced tumor burden due to improved therapy assessment.

## 1.2 Common Genomic Alterations and Relevant Targeted Therapies

EGC is a heterogeneous disease with many identified genes implicated in disease progression. As mentioned earlier, there is *intra*-tumor variability which creates a major barrier for targeted therapies, but *inter*-tumor variability also offers a major barrier as all patients present with a vast and unique genetic landscape. We will explore a number of common EGC-causing mutations and corresponding targeted therapies that have been investigated.

### 1.2.1 HER2

HER2 (also known as ERBB2) is a proto-oncogenic receptor tyrosine kinase (RTK) that regulates signals from growth factors and stimulates cellular pathways involved in proliferation and survival. HER2 is overexpressed in approximately 18% of EGC's, although this number varies from 4% to 53% depending on patient datasets[30]. HER2 maintains a controversial prognostic value with several people arguing HER2 positivity has no impact on patient survival, although others claim that HER2-positive tumors show increased aggressiveness and recurrence rates[37,38].

As discussed earlier, HER2 inhibitors are among the only successful targeted therapies currently being used in EGC patients. The ToGA study was an open-labelled phase III clinical trial where 594 patients from 122 centers across 24 countries were randomly assigned into two main groups: trastuzumab + chemotherapy (capecitabine and cisplatin or 5-FU) or chemotherapy

alone. The 594 selected patients were confirmed for HER2 'positivity' (overexpression) by immunohistochemical analysis. The study was able to find a statistically significant increase in OS from 11.1 months to 13.8 months in the combination group, directing trastuzumab plus chemotherapy as a valid first-line therapy for HER2-positive gastric tumors[31]. Nonetheless, the clinical significance is moderate at best and has a far lower survival benefit than HER2-directed therapies in breast cancer[39].

Trastuzumab based therapies are currently the only approved targeted treatment options for HER2-positive gastric cancers[31]. The LOGiC phase II clinical trial investigated the efficacy of lapatinib, a dual HER2 and EGFR inhibitor in HER2-positive EGC patients. 545 patients were randomly assigned to lapatinib plus chemotherapy (capecitabine and oxaliplatin) or chemotherapy alone, although no significant difference in median survival was observed[40]. Lapatinib plus capecitabine showed promising results in HER2-positive breast cancer patients[41]. The lapatinib plus chemo group in the LOGiC study showed significantly more adverse effects and a greater rate of treatment discontinuation than the lapatinib plus chemo group in the breast cancer trials. Many hypothesize the chemotherapy backbone in the LOGiC trial led to reduced treatment efficacy[39]. Lapatinib monotherapies are currently being evaluated in phase II/III clinical trials (NCT02250209).

Pertuzumab is a monoclonal antibody which targets a different epitope of HER2 than trastuzumab, and has shown clinical significance when combined with trastuzumab in breast cancer patients[42]. The JACOB study was a phase III clinical trial investigating pertuzumab plus trastuzumab and chemotherapy versus trastuzumab and chemotherapy alone in HER2-positive metastatic gastric tumors. In contrast to breast studies, the JACOB study confirmed no significant impact of adding pertuzumab to trastuzumab-based therapies in EGC[43]. These among

other failed HER2-directed clinical trials in EGC may be attributed to HER2 heterogeneity, as well as different mechanisms of signalling regulation compared to breast cancer[39].

### 1.2.2 VEGFR

Tumor angiogenesis and lymphangiogenesis are considered major driver events in metastasis. The proliferation of blood and lymphatic vessels supplies the tumor with a favorable nutrient-rich microenvironment to sustain growth and promote tumor cell invasion. Vascular endothelial growth factors (VEGF-A, VEGF-B, VEGF-C, VEGF-D, VEGF-E, VEGF-F) are among the most important factors promoting tumor angiogenesis and function through VEGF receptors (VEGFR1, VEGFR2, VEGFR3), a specific type of RTK found on endothelial cells[44]. VEGFR's are overexpressed in approximately 36-40% of gastric tumors[45]. Prognosis is largely based on the tumoral expression profiles of VEGF's and VEGFR's. Most notably, overexpression of VEGFR2 and VEGFR3, especially with high circulating levels of VEGF-C and VEGF-D have been implicative of poor prognosis in gastric cancer[46,47].

Angiogenesis inhibitors have been under extensive investigation as anti-cancer therapies, attempting to inhibit tumor growth by blocking blood vessel formation. The REGARD study, a phase III clinical trial, demonstrated the clinical efficacy of VEGFR inhibition as a second-line therapeutic strategy in gastric cancer[48]. In the study, 355 GEJ and GA patients across 119 centers worldwide who had previously received first-line platinum-based or fluoropyrimidine-containing chemotherapy were randomly assigned into two groups; both given best supportive care with or without ramucirumab, a monoclonal antibody against VEGFR2. Investigators concluded that the patients given ramucirumab demonstrated a median OS of 5.2 months, in comparison to the placebo subgroup with a median OS of 3.8 months[48]. Similarly, the RAINBOW trial showed

comparable results in gastric and GEJ cancer patients who had progressed after first-line chemotherapy. They concluded that second-line treatment of ramucirumab plus paclitaxel significantly improved OS (9.6 months) compared to placebo plus paclitaxel (7.4 months)[49].

Trastuzumab and ramucirumab are currently the only two targeted therapies approved for EGC patients, although trastuzumab is the only therapy approved for first-line treatment. Although trastuzumab has exhibited clinical value for HER2-positive EGC patients, many patients still progress during first-line treatment with trastuzumab[50]. A randomized phase II study of gastric and GEJ cancer patients who had progressed during first-line trastuzumab therapy proved that further administration of trastuzumab plus paclitaxel showed no survival benefit compared to paclitaxel alone[51]. A recent subgroup analysis on the RAINBOW trial showed that patients who had progressed following first-line trastuzumab therapy showed higher OS in the ramucirumab group (11.4 months) compared to the placebo group (7.0 months)[52].

The AVAGAST phase III clinical trial attempted to identify VEGF-A as a potential target. Investigators randomly assigned gastric cancer patients for first-line treatment of chemotherapy plus bevacizumab, a monoclonal antibody against VEGF-A, or chemotherapy alone (capecitabine and cisplatin) and concluded no significant differences in OS, although they observed an advantage in progression free survival (PFS)[53]. Similarly, second-line bevacizumab-based treatments have shown uninspiring results in EGC[54].

There are currently many ongoing clinical trials involving VEGFR tyrosine kinase inhibitors (TKI). Most notably, the selective VEGFR2 inhibitor Apatinib, is shown to be an effective third-line treatment option for advanced or metastatic gastric and GEJ adenocarcinoma patients who progressed after first- or second-line chemotherapy[50,55].

### 1.2.3 EGFR

Epidermal growth factor receptor (EGFR) is a HER-family RTK involved in transducing signals from growth factors, most notably the epidermal growth factor (EGF)[56]. EGFR activation affects numerous signalling pathways involved in cellular proliferation, differentiation, migration and survival, such as the mitogen-activated protein kinase (MAPK) and phosphoinositide 3-kinase-AKT (PI3K/AKT) pathways. Approximately 27% of EGC patients express an EGFR mutation, although this number varies extensively in the literature[57,58]. EGFR overexpression in GA patients is often associated with a poorer prognosis[58,59]. EGFR detection by immunohistochemical (IHC) analysis has been linked to lymph node metastasis, advanced stage and poor survival[58].

EGFR inhibitors have been extensively studied as targeted therapeutics for EGC patients. Monoclonal antibodies directed against EGFR were first investigated but showed little clinical significance. The EXPAND study, a phase III clinical trial, investigated Cetuximab in combination with cisplatin and capecitabine, while the REAL3 trial inspected Panitumumab in combination with epirubicin, oxaliplatin and capecitabine. Both trials showed no improvement in PFS or OS[60,61]. Furthermore, second-line gefitinib monotherapies were evaluated in a phase III clinical trial (COG trial) for gastric cancer patients, where results showed no clinical benefit[62]. One of the biggest critiques of these trials, along with many other targeted therapy studies, is the lack of mutational screening prior to treatment. This is in contrast to many HER2 studies, which identified HER2-directed therapies that benefit HER2-positive EGCs[63]. Although the COG trial showed no overall survival benefit for gastric cancer patients, could it provide clinical utility to patients with EGFR overexpression? *Post-hoc* molecular analysis of COG trial tumors by fluorescent insitu hybridization (FISH) looked to identify EGFR copy number gain. They were

able to identify a subgroup of patients with high EGFR copy number gain (>4) that showed a statistically significant survival benefit to second-line gefitinib monotherapy[64]. Similar *post-hoc* analyses on the EXPAND and REAL3 trials showed a potential survival benefit for cetuximab and panitumumab for EGFR-overexpressing tumors[65,66]. As of now, EGFR antibodies and inhibitors have yet to show any clinical utility, although further investigation is required to analyze their value under proper patient stratification procedures.

### 1.2.4 FGFR

Fibroblast growth factor receptors (FGFR1, FGRF2, FGRF3, FGFR4) are a superfamily of RTKs, which function similarly to other RTKs such as EGFR. Binding of FGF ligand to the receptor causes dimerization and autophosphorylation of tyrosine residues on the receptor's cytoplasmic domain. This causes subsequent activation of downstream signalling pathways such as the MAPK and PI3K pathways, which promote cell growth, proliferation and survival[67]. FGFR2 is the most commonly amplified FGFR receptor, where it's overexpressed in approximately 10% of gastric tumors[68]. FGFR amplification has been associated with poorer prognosis and lymphatic invasion[68-70].

There has been a rise in the development of FGFR inhibitors to test FGFRs as druggable candidates. Pre-clinical models were used to assess the efficacy of these inhibitors *in vitro* and *in vivo*. One study found that gastric cancer cell lines with amplification of FGFR2 (SNU-16 and KATOIII) were significantly more sensitive to the FGFR1-2-3 inhibitor AZD4547, compared to non-amplified tumors[71]. These results were further evaluated in patient-derived xenograft (PDX) models (SNU-16), whereby investigators concluded that the AZD4547 inhibitor in combination with paclitaxel demonstrated the largest anti-tumor effects[71]. Nonetheless, the efficacy of

AZD4547 was not found to be significant in the SHINE phase II clinical trial, which showed that FGFR-amplified GA patients did not benefit from second-line treatment with AZD4547 in comparison to paclitaxel[34]. Other FGFR-targeted therapies that have shown promise in preclinical models are currently being investigated in ongoing clinical trials[72].

### 1.2.5 MET

The hepatocyte growth factor (HGF) is the primary ligand of the HGF receptor, commonly known as MET (MNNG-HOS transforming gene), which not only supports proliferative and antiapoptotic roles through MAPK and PI3K pathways, but also functions in promoting cell-cell detachment and migration[73]. MET amplification is identified in 2-10% of EGC's and often indicates poor prognosis[74,75]. MET overexpression is associated with tumor invasion, distant metastasis, lymph node metastasis and overall poor survival[75].

Over the last decade there has been a substantial amount of investigation into anti-MET targeted therapies using monoclonal antibodies and TKIs for EGC. The RILOMET-1 study, a phase III clinical trial looked at the effect of adding rilotumumab, an antagonistic monoclonal antibody of MET, to standard ECX therapy (epirubicin, cisplatin and capecitabine)[35]. The multicenter trial randomly assigned 609 HER2-negative, MET-positive GA patients to receive rilotumumab plus ECX or placebo plus ECX. They concluded that rilotumumab was not successful at improving clinical outcome in MET-positive gastric tumors[35]. In fact, the RILOMET-1 trial was suspended early due to a disproportionate number of deaths and a lower PFS and OS in the rilotumumab group. Similarly, the METgastric phase III study concluded that the anti-MET monoclonal antibody onartuzumab (in combination with mFOLFOX6) was ineffective at improving survival outcome, even in MET-positive tumors[76]. There are a number

of anti-MET TKIs that have been examined as well, although none have shown clinical significance. For example, foretinib is a dual MET and VEGFR2 inhibitor which showed promise in preclinical models by inhibiting gastric cancer cell growth, failed to show any clinical significance in a phase II trial for metastatic gastric cancer patients[77,78].

### 1.2.6 MAPK Pathway

The MAPK signalling pathway, consists of a chain of proteins, RAS-RAF-MEK-ERK, which transduce extracellular signals, commonly from growth factors acting on RTKs to the nucleus to regulate gene expression, metabolism, cell proliferation, apoptosis, among other functions[79]. Abnormal MAPK pathway activation has been implicated in the progression of many cancers and neurodegenerative diseases. Hyperactivation of the MAPK pathway can arise from irregular amplification of RTKs or may be due to oncogenic mutations in the proteins comprising the pathway itself, most notably mutations in KRAS (Kristen rat sarcoma 2 viral oncogene homolog) and BRAF (Raf murine sarcoma viral oncogene homolog B) proteins[80]. BRAF mutations are infrequent in gastric cancers with an incidence of only 2%, where most mutations are not located at the mutational hotspot V600, which is commonly identified in colorectal cancer[81]. Similarly, KRAS mutations are found in 6.5% of gastric cancers (on average) compared to 25% in other cancer subtypes[82]. The mutational backgrounds of BRAF and KRAS are still poorly understood in gastric cancer, but it is thought that RTK and MEK alterations are the main drivers for MAPK pathway hyper-amplification.

Due to the central role of the MAPK pathway in cancer progression, many have sought to target its components. There are currently three FDA-approved drugs available for patients with nonresectable or metastatic melanoma. Vemurafenib, a BRAF inhibitor, showed successful

results in a phase II clinical trial comparing its effects to dacarbazine in melanoma patients with a BRAF V600 mutation[83]. Similarly, metastatic melanoma patients with $BRAF^{V600E}$ mutation showed better PFS and OS when administered the BRAF inhibitor dabrafenib, compared to dacarbazine[84]. Combination therapy using dabrafenib and the MEK inhibitor trametinib outperformed dabrafenib monotherapy in three phase III clinical trials and is currently the standard of care for metastatic melanoma patients[85,86]. A recent phase I clinical trial for patients with advanced solid tumors and MAPK alterations, showed promising results for the ERK1/2 inhibitor ulixertinib[87]. There remains little known on the value of MAPK pathway targeting agents in EGC.

Although MAPK pathway targeting provides clinical utility in certain cancer types, there is a large proportion of patients who develop resistance to therapies. This is mainly due to upregulation of other components in the pathway, such as enhanced KRAS activity or EGFR phosphorylation or of other pathways such as the PI3K/AKT pathway[86,88]. *In vitro* and *in vivo* models of EGC discovered a potential mechanism to overcome KRAS-mediated MAPK resistance[89]. MAPK blockade in KRAS wild type (WT) tumors promoted an adaptive response, shifting KRAS into its GTP-bound state via SHP2 and SOS1/2. Investigators determined that inhibiting the protein tyrosine phosphatase SHP2, in KRAS WT gastric tumor cells, increased their sensitivity to MEK inhibition and could provide a mechanism for overcoming resistance[89].

### 1.2.7 PI3K Pathway

The PI3K pathway is activated in an analogous manner to the MAPK pathway, commonly by growth factors activating RTKs or G protein coupled receptors (GPCRs). Phosphatidylinositol-3-kinase (PI3K) exists as a heterodimer comprised of regulatory subunit

(p85) and a catalytic subunit (p110)[90]. PI3K activation via RTKs or GPCRs leads to the initial phosphorylation of phosphoinositide-dependent kinase 1 (PDK1), which in turn creates a cascade of protein phosphorylation, with notable players like AKT and mTOR (mammalian target of rapamycin)[90]. AKT phosphorylation by PDK1 or PDK2 phosphorylates many downstream targets including mTOR. mTOR activates the eukaryotic initiation factor 4E (4EBP1) and ribosomal S6 protein (S6K1). Downstream effectors of the pathway modulate gene transcription, cell growth, apoptosis and proliferation. Like the MAPK pathway, the PI3K pathway has been implicated in tumorigenesis when dysregulated, which could be due to a number of factors such as hyperactivation of RTKs, mutations in pathway components such as PIK3CA, AKT or mTOR, or as a compensatory measure[91].

The PI3K pathway is the second most frequently altered pathway in human cancers, after the p53 pathway[92]. In gastric cancer, PIK3CA is the most commonly mutated gene in the PI3K pathway, with an alteration frequency of 18%[90]. The majority of PIK3CA mutations are found in EBV-positive EGCs[27]. 80% of these mutations occur at three main hotspots: E545K and E542K of exon 9 and H1047R in exon 20, all of which are associated with poor prognosis[93,94]. Alteration frequencies in other isoforms (PIK3CB and PIK3CD) are quite rare[90]. mTOR is mutated in approximately 4% of gastric cancer patients[90]. AKT isoforms (AKT1, AKT2, AKT3) are mutated in only 1-3% of gastric tumors, although IHC analysis showed AKT overexpressed in up to 74%[90,95]. AKT1 functions primarily in cellular proliferation and survival, whereas AKT2 promotes for cellular invasiveness and increases metastatic potential. AKT3 is rarely expressed in the stomach[90].

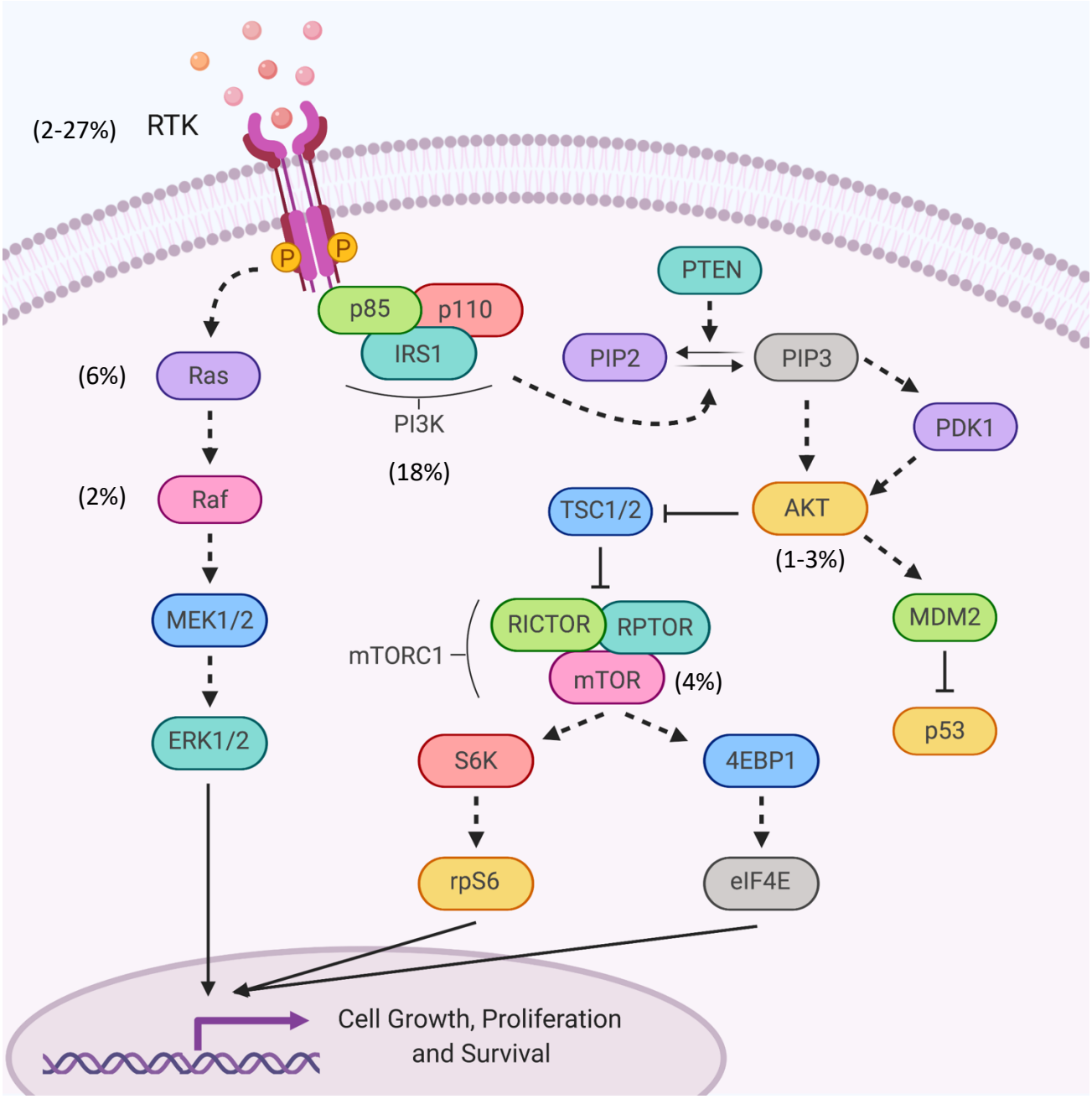


**Figure 1: Summary of MAPK and PI3K Pathways.** Highlighting the major components of the MAPK (left) and PI3K (right) pathways. Alteration frequency in EGCs (in %) is listed for selected genes (RTKs, KRAS, BRAF, PIK3CA, AKT and mTOR).

The PI3K pathway has been actively investigated to identify clinically effective druggable targets. There are four main classes of inhibitors that target the PI3K pathway: PI3K inhibitors, mTOR inhibitors, dual PI3K/mTOR inhibitors and AKT inhibitors. The GRANITE-1 phase III clinical trial was the first major study of targeting the PI3K pathway in gastric cancer[96]. Gastric cancer patients were given everolimus, an mTOR inhibitor, as a second-line therapy in combination with best supportive care. However, everolimus treated patients did not show any improvements in median OS[96]. This may be attributed to the fact that patients were not pre-selected based on PI3K/AKT/mTOR alterations. Similarly, the SWOG trial concluded that the AKT inhibitor MK-2206 as second-line therapy provided little improvement in clinical outcome (response rate of 1%)[97]. There are several ongoing clinical trials for PI3K pathway targeted therapies, many of which are supported by preclinical evidence[90]. For example, the dual PI3K/mTOR inhibitor BEZ235 showed significant anti-tumor activity in paclitaxel-resistant cell lines and tumor bearing mouse models[98].

### 1.2.8 ARID1A

AT-rich interactive domain 1A (ARID1A) is a tumor suppressor involved in the epigenetic modulation of gene expression. It is a key component of the SWItch/Sucrose Non-Fermenting (SWI/SNF) complex, serving specific roles in chromatin remodeling. ARID1A acts as the 'DNA sensor,' interacting with specific DNA sequences to be remodelled by other proteins in the complex to modulate DNA accessibility[99,100]. ARID1A has an alteration frequency of 8-33% in EGCs and is typically associated with loss of function[101]. ARID1A loss is associated with lymphatic invasion, lymph node metastasis and poor survival prognosis[102]. Loss of ARID1A

expression typically co-occurs with activating mutations of PIK3CA in gastric and other types of cancers, although the underlying mechanisms remain unclear[103].

*In vivo* ovarian clear cell carcinoma (OCCC) models found that ARID1A inactivation was insufficient to promote tumor formation[104]. However, when ARID1A loss occurred concurrently with PIK3CA activation, tumorigenesis followed. The same study showed that subsequent induction of the PI3K inhibitor BKM120 slowed tumor growth and prolonged mouse survival[104]. In spite of the high incidence of ARID1A mutations, clinical therapies are not yet available. Many propose ARID1A as a synthetic lethal candidate for other genomic alterations, thereby suggesting that the presence of an ARID1A mutation may sensitize the tumor to other targeted therapies[105]. Some proposed synthetic lethal candidates include the DNA damage checkpoint kinase ATR, other epigenetic targets such as the histone deacetylase 6 (HDAC6) or enhancer of zeste homolog 2 (EZH2) and many targets of the PI3K pathway such as PIK3CA and AKT[105,106]. For example, an *in vitro* study was able to identify the AKT inhibitor GSK690693 as a potential therapeutic strategy in ARID1A-mutant gastric tumors. ARID1A-knockdown in gastric cancer cell lines (MKN-1, MKN-28 and KATO-III) resulted in increased sensitivity to GSK690693 plus cisplatin or 5-FU, compared to controls[107].

### 1.2.9 Exploring Combination Therapies

Currently BRAF and ERK targeted therapies result in developed resistance in about half of patients[86]. Similarly, although PI3K pathway inhibitors are promising, it is still too early to predict their success in the clinic, especially as monotherapies. Several studies have questioned the potential efficacy of monotherapies against the PI3K pathway, which has been shown to not be the case for MAPK signalling inhibitors. These uncertainties are due to the presence of

positive feedback loops, compensatory mechanisms and the dual tumorigenic roles of the PI3K and MAPK pathways[90]. These observations have guided us into the era of combination therapies.

An important aspect of combination therapies is the notion of how drugs interact. Different drugs can interact in unexpected ways and yield substantially different outcomes. Some drugs show antagonistic roles, whereby the presence of both drugs dampens their effects, but this is typically undesirable. Researchers strive to find synergistic drug combinations, where due to the biochemical characteristics of the drugs, potentiate and show enhanced efficacy when combined[108].

One *in vivo* study in a murine lung adenocarcinoma model, showed that KRAS-mutant lung cancers were resistant to the BEZ235 PI3K inhibitor and to the ARRY-142886 MEK inhibitor. When given in combination however, they expressed synergism and were effective at reducing tumor volume[109]. Another *in vivo* study using KRAS-mutant colorectal cancer models, demonstrated that the EGFR inhibitor dacomitinib was sufficient to relieve the acquired resistance of the PI3K/mTOR inhibitor PF-04691502 when administered in combination. Both dacomitinib and PF-04691502 showed limited efficacy as single-agent therapies[110]. Similarly, *in vitro* and *in vivo* studies in OCCC identified synergistic activity between the PI3K/mTOR inhibitor PF-04691502 and the MEK inhibitor PD-0325901[111]. As alluded to throughout this literature review, combination therapies are not novel, as most targeted therapies are given in combination with chemotherapy regimens. That being said, combining targeted treatments, especially those between the MAPK and PI3K pathways, could be a therapeutic approach to overcoming drug resistance due to analogous downstream effects.

| Target | Agent | Trial | Clinical Trial Design | Survival Benefit (Experimental vs. Control, in Months) |
|---|---|---|---|---|
| HER2 | Trastuzumab | ToGA; Phase III | Chemotherapy ± Trastuzumab 1st line | Positive (13.8 vs. 11.1) |
| | Lapatinib | LoGIC; Phase II[40] | Chemotherapy ± Lapatinib 1st line | Negative (12.2 vs. 10.5) |
| | Lapatinib | TyTAN; Phase III[32] | Paclitaxel ± Lapatinib 2nd line | Negative (11.0 vs. 8.9) |
| | Pertuzumab | JACOB; Phase III[43] | Chemotherapy and Trastuzumab ± Pertuzumab 1st line | Negative (17.5 vs. 14.2) |
| VEGFR | Ramucirumab | REGARD; Phase III[48] | Chemotherapy ± Ramucirumab 2nd line | Positive (5.2 vs. 3.8) |
| | Ramucirumab | RAINBOW; Phase III[49] | Paclitaxel ± Ramucirumab 2nd line | Positive (9.6 vs. 7.4) |
| | Apatinib | NCT01512745; Phase III[55] | Apatinib vs. Placebo 3rd line | Positive (6.5 vs. 4.7) |
| VEGF | Bevacizumab | AVAGAST; Phase III[53] | Chemotherapy ± Bevacizumab 2nd line | Negative (12.1 vs. 10.1) |
| FGFR | AZD4547 | SHINE; Phase II[34] | AZD4547 vs. Paclitaxel 2nd line | Negative (1.8 vs. 3.5) |

**Table 1: Summary of completed targeted therapy clinical trials in EGC.** Highlights the most important clinical trials in EGC for targeted therapies. Table lists the target, drug used, trial name and design as well as results in terms of survival benefit

| Target | Agent | Trial | Clinical Trial Design | Survival Benefit (Experimental vs. Control, in Months) |
|---|---|---|---|---|
| EGFR | Cetuximab | EXPAND; Phase III[60] | Chemotherapy ± Cetuximab 1st line | Negative (9.4 vs. 10.7) |
| | Panitumumab | REAL3; Phase III[61] | Chemotherapy ± Panitumumab 1st line | Negative (8.8 vs. 11.3) |
| | Gefitinib | COG; Phase III[62] | Gefitinib vs. Placebo 2nd line | Negative (3.7 vs. 3.7) |
| MET | Rilotumumab | RILOMET-1; Phase III[35] | Chemotherapy ± Rilotumumab 1st line | Negative (8.8 vs. 10.7) |
| | Onartuzumab | METgastric; Phase III[76] | mFOLFOX6 ± Onartuzumab 1st line | Negative (11.0 vs. 11.3) |
| MTOR | Everolimus | GRANITE-1; Phase III[96] | Chemotherapy ± Everolimus 2nd line | Negative (5.4 vs. 4.3) |
| PD-1/PDL-1 | Nivolumab | ATTRACTION-2; Phase III[23] | Nivolumab vs. Placebo 2nd line | Positive (5.3 vs. 4.1) |
| | Pembrolizumab | KEYNOTE-061; Phase III[25] | Pembrolizumab vs. Paclitaxel 2nd line | Negative (9.1 vs. 8.3) |
| | Ipilimumab | NCT01585987; Phase II[26] | Ipilimumab vs. Chemotherapy 2nd line | Negative (2.9 vs. 4.9) |

**Table 1 continued: Summary of completed targeted therapy clinical trials in EGC.** Highlights the most important clinical trials in EGC for targeted therapies. Table lists the target, drug used, trial name and design as well as results in terms of survival

## 1.3 Patient-Derived Organoids as Preclinical Models for Drug Testing

The cost associated with the research and development of a novel cancer therapy drug, from the induction of preclinical studies until its approval by the United States Food and Drug Administration (FDA) for clinical use is approximately 648 million dollars[112]. The average time it takes for a drug to be approved by the FDA ranges from 5 to 15 years[113]. This costly and lengthy period for drug development highlights the demand for finding improved preclinical models. Most notably, patient-derived organoids (PDOs) have shown promise at improving the efficiency of drug development and will be the central focus for the remainder of this review.

### 1.3.1 Generating and Maintaining PDOs

Organoids are microscopic three-dimensional structures *in vitro*, which recapitulate many features of the original *in vivo* tissue. Surgically resected and biopsied tumor samples from EGC patients are digested into single cells, which are resuspended in a gelatinous matrix called Matrigel, a basement membrane matrix from mouse tumors that consists of extracellular matrix components like collagen, laminin and enactin[114]. Matrigel provides a suitable environment for cells to proliferate in a three-dimensional manner, forming spherical cell structures. Gastric organoid medium is added to Matrigel-embedded organoids and contains a wide variety of growth factors, such as Wnt3A, R-spondin and Noggin, which promote gastric epithelial cell proliferation[113].

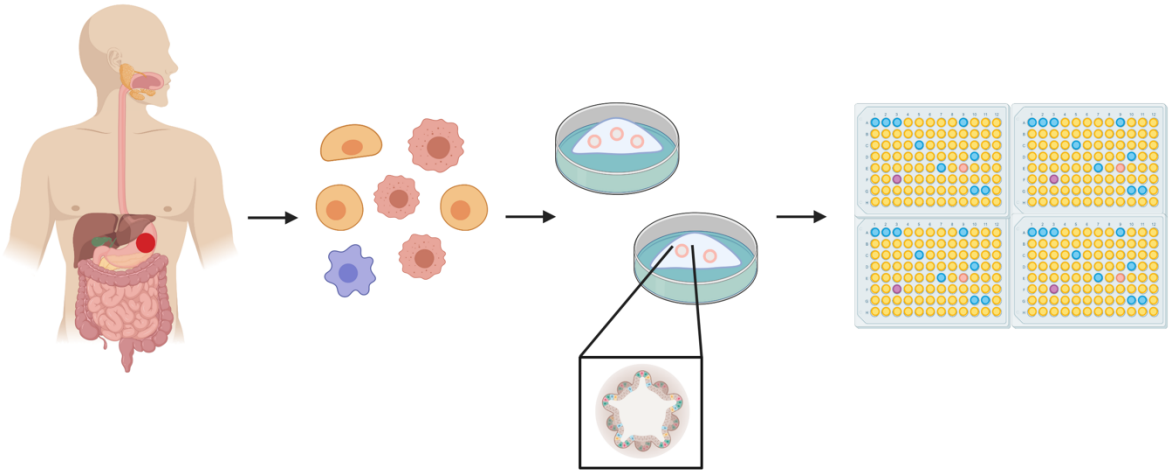

**Figure 2: Preparing organoids from primary patient material or PDXs creates a heterogenous cell population.** Organoids are composed of a variety of cell types from the initial tumor. Single cells are cultured in domes of Matrigel, which forms a varied 3-dimensional organoid population which can be used to perform high-throughput drug screens.

### 1.3.2 Organoids as Alternatives to Cancer Cell Lines and PDXs

Over the last few decades, cancer cell lines (CCLs) and PDX models have dominated the sphere of cancer research. Gastric organoids were first established in 2010 to model the self-renewal capacity of Lgr5$^{+ve}$ stem cells of the pyloric epithelium[115]. Since then, organoids have served an essential role in modeling cancer.

Although easy to maintain and rapid to develop, CCLs are not suitable cancer models as they lack the structural and genetic characteristics of the original tumor. CCLs have been criticized for their inability to recapitulate the genetic landscape of the original tumor. For example, one study identified that hypoxic conditions given to four 'identical' HeLa cell lines resulted in activation of different pathways and transcriptomic variability, concluding

irreproducible results[116]. Gastric tumor organoids are better able to recapitulate *intra*-patient heterogeneity and maintain a genomic landscape representative of the patient's original tumor[117]. PDOs from gastric tumor biopsies were able to show comparable genomic alterations, even after serial passages[117]. Unlike CCLs, PDOs are composed of a diverse cell population, which is more replicative of the tumor itself[118]. Similarly, PDOs better capture *inter*-patient heterogeneity, making them useful models for drug assays.

Patient derived xenografts (PDXs) are generated from the subcutaneous or orthotopic implantation of patient material. Unlike CCLs, PDXs are better able to maintain structural and genomic integrity of the primary tumor. PDXs also contain components of the tumor microenvironment (TME) which are largely absent in PDOs, although organoid co-cultures with immune cells and other aspects of the TME have begun extensive investigation[119,120]. Similar to CCLs, PDOs can be readily transplanted into immunodeficient mice to promote tumor growth[121]. These *in vivo* methods remain a gold standard for drug testing but are rather limited by high costs and prolonged periods for tumor growth. PDOs are more fitting as cancer models, especially in instances of patient drug assessment, as they can be developed within a shorter time period, usually in the span of a month[113].

PDOs are a valuable tool for tracking the tumorigenic stages of the disease. One study was able to identify both similarities and differences in gene expression between organoids derived from dysplasia tissue (at the edge of the tumor) and from the invasive tumor itself of the same patient[122]. For example, common patterns of expression were observed with TP53 and APC, whereas BAX and TSC1 were mutated solely in the dysplasia and SMARCA4 and STK11 mutations were found exclusively in the invasive tumor[122]. Similar studies have compared the chromosomal profiles of the primary tumor to the metastatic disease using PDOs[123]. Organoids

can also be manipulated in such a way as to model cancer progression. Normal patient tissue can be used to derived organoids *in vitro* and allow for further manipulation to track tumorigenesis. CRISPR/Cas9 targeted quadruple knockout of KRAS, APC, SMAD4 and P53 performed on normal intestinal organoids promoted tumor formation following xenotransplantation into mice[124].

### 1.3.3 Organoids as Models of Predictive and Personalized Medicine

One major desired outcome of organoid research is to use PDOs as a prognostic factor, to predict patient response to treatment. Many patients respond to chemotherapy and targeted agents with varying efficacies, potentially due to their genetics. Many studies have been successful at retrospectively matching PDO response to the patient's initial response to therapy[120,125,126]. One such study derived a PDO biobank for pancreatic cancer patients and identified two cohorts based on transcriptional signatures[126]. They were capable of clumping similar responders to treatment into each transcriptional cohort and identified a group of patients with substantially better response to chemotherapy[126]. Lapatinib, the dual EGFR and HER2 inhibitor is currently approved for treating metastatic breast cancer in combination with capecitabine[127]. One study was able to identify a subset of gastric PDOs that responded well to lapatinib. ERBB2-overexpressing PDOs showed increased sensitivity to lapatinib compared to ERBB2 wild type gastric tumor organoids[125]. In the same study, a gastric cancer organoid line with AKT1 mutation showed enhanced sensitivity to the AKT inhibitor MK-2206[125].

PDOs demonstrate potential for clinical use to predict patient response to chemotherapy and other personalised targeted therapies. PDOs grow quickly and in large quantities sufficient to perform high-throughput drug screens on a wide variety of therapeutic agents. These organoids

can be used to identify therapies based on genomic alterations. PDOs may also be useful in identifying salvage therapies for patients who develop resistance to first-line therapies. The OPPOSITE clinical trial (NCT03429816) is undergoing a large-scale study in EGC, where patient's tumor at time of biopsy (pre-neoadjuvant therapy) and after neoadjuvant systemic therapy will be used to generate PDOs. These organoids will be used to validate patient response to treatment *in vitro*. The study aims to correlate the patient's response to therapy with the organoid's response *in vitro,* on a large scale. The main objective is to be able to use PDOs in the laboratory as a clinical test to discover personalized therapeutic options for the patient, based on the organoids response to said treatment.

### 1.4 Project Rationale and Objectives

EGCs are associated with high mortality and morbidity rates, creating a major burden on patients diagnosed with the disease. Current standard-of-care fails to consider a patient's genomic background, which results in suboptimal response rates. With the knowledge of inter-patient genomic heterogeneity and the co-occurrence of alterations in multiple genes, it would be a valuable approach to identify targeted therapies guided by genomic testing for EGC patients. ARID1A loss is common in EGC and often co-occurs with activating mutations of the PI3K and MAPK pathways. ARID1A has previously been proposed as a synthetic lethal candidate for PI3K/Akt/mTOR pathway targeting agents, although its role as a biomarker has yet to be investigated in EGC. Our lab has generated a unique PDX cohort from 33 EGA patients, of which organoids can be derived from. Genetic profiling of our PDXs along with *in vitro* high-throughput drug screening on matched organoids allows us to compare drug response to genomic

background. The overall aim of this project is to identify potential targeted therapies in ARID1A-mutant organoids, specifically investigating PI3K and MAPK pathway components. We sought to:

a. Identify the ARID1A alteration frequency in our PDX cohort, while investigating commonly co-occurring alterations.
b. Compare the protein expression levels from PDX lysates to their corresponding genomic profiles.
c. Perform *in vitro* high-throughput drug screening on a number of PDX-derived organoid lines, with specific attention to PI3K and MAPK pathway targeting agents.

# CHAPTER 2: MATERIALS AND METHODS

## 2.1 Patient Material Collection

Gastric and esophageal cancer tissues were obtained from consenting patients undergoing endoscopy or surgical resection at the Montreal General Hospital (MGH). All tissue was collected as per Institutional Review Board guidelines at the McGill University Health Center (MUHC-REB protocol #2007-856).

## 2.2 Patient-derived xenografts

Primary patient tumors from consented esophago-gastric cancer patients were subcutaneously implanted into immunocompromised NSG mice. Tumor size was measured once a week. Once tumor volume reached 300mm$^3$, mice were sacrificed, and tumor tissue was passaged into 2 new animals. A piece of the excised tumor was also used to derive organoid cultures. All experiments were conducted with the approval of and in agreement with the guidelines of the McGill University Animal Care Committee.

## 2.3 Generating PDX-derived organoids

Tumor pieces from a PDX were digested to obtain single cells using the tumor dissociation kit from MACS Miltenyi Biotech. Tissue was chopped by hand into fine pieces and added to gentleMACS C Tubes (Miltenyi, 5190415004) containing DMEM and the R, H and A enzymes from the tumor dissociation kit for chemical disruption. The gentleMACS Octo Dissociator was used for further mechanical disruption. Once digested, the cells were passed through a 70μm filter and washed with 10mL of PBS (Gibco, 14190-144). Cells were

centrifuged at 1200rpm for 4min and the supernatant was removed. If red blood cells were visible in the pellet, 1-2mL of ACK Lysis Buffer (Gibco, A10492) was added for 3 minutes. Cells were centrifuged again, and the supernatant was replaced with a solution of Mouse cell depletion cocktail (MACS Miltenyi Biotech, 130-104-694). The MACS Multistand apparatus using LS columns (MACS Miltenyi Biotech, 130-042-401) was used to eliminate any mouse-derived cells. Cell count and viability was performed using the Countess II FL, whereby cells were diluted by half in 0.4% Trypan Blue solution (Gibco, 15250-061) and imaged on Countess cell counting chamber slides (Invitrogen, C10283). NUNC Multidish 12-well plates (Thermo, 150628) were coated with a layer of Matrigel (Corning, 356231) and stored in a 37°C incubator for 30 minutes. Complete gastric organoid medium was prepared by adding gastric organoid media[128] to completed human IntestiCult (composed of components A (Stemcell, 06011) and B (Stemcell, 06012)). Complete gastric organoid media supplemented with 5% Matrigel was mixed with single cells. 100,000 cells were seeded per well in the Matrigel-coated 12-well plate. Cells were stored in a HERAcell V10S 160i, $CO_2$ incubator by Thermo scientific at 37°C, 5% $CO_2$ and 3% $O_2$.

**2.4 Organoid Culture**

Complete gastric organoid media (+ 5% Matrigel) was replenished every 3 days and cells were kept in culture for approximately 1-2 weeks or until organoids reached sufficient size. Once fully grown, organoids were expanded or frozen down. Organoid medium was replaced with a solution of collaganse/dispase (Roche, 10269638001/11097113001) in Dulbecco's Modified Eagle Medium (Gibco, 11995-065) and stored in a $CO_2$ incubator for up to 2 hours. Once the matrix was degraded, organoids were transferred to a 15mL canonical tube and centrifuged at

1200rpm for 4 minutes. Supernatant was replaced with 1mL of 0.25% trypsin (Gibco, 15050-065) to dissociate the organoids into single cells. Digestion was stopped after organoids were disrupted into single cells by adding 10mL of 90% DMEM + 10% FBS (Gibco, 12483-020). Cells were centrifuged and supernatant was replaced with complete gastric organoid media. Cell count and viability was measured using Countess II FL and appropriate number of cells were seeded as mentioned earlier. Excess cells were added to 1mL of 90% FBS + 10% DMSO in CryoPure tubes (Sarstedt, 9081911) and placed in a CoolCell LX at -80°C (Corning, 432002). Cells were stored long-term in liquid nitrogen.

**2.5 Preparing drug stocks**

All drugs (except Cisplatin) were diluted in Dimethyl sulfoxide (DMSO; Sigma, SHBL2891) to a concentration of 10mM and stored short-term at -20°C or long-term at -80°C. The drugs prepared and used in the drug screen include: Docetaxel (Cayman, 11637), 5-Fluorouriacil (Cayman, 14416), EZH2 inhibitor UNC1999 (Cayman, 14621), EGFR inhibitor Gefitinib (Cayman, 13166), MET inhibitor Crizotinib (Cayman, 12087), VEGFR inhibitor Sorafenib (Cayman, 10009644), BRAF inhibitor Dabrafenib (Cayman, 16989), MEK inhibitor Trametinib (Cayman, 16292), ERK1/2 inhibitor Ulixertinib (Cayman, 18298), dual PI3K/mTOR inhibitor Gedatolisib (Cayman, 14567), PIK3CA inhibitor Alpelisib (Cayman, 16986), PIK3CG inhibitor Duvelisib (Cayman, 16800), mTOR inhibitor Sirolimus (Cayman, 13346) and AKT1/2 inhibitor Uprosertib (Cayman, 19904). Cisplatin (Cayman, 13119) was prepared in pre-heated 0.9% saline at a concentration of 4mM. Frequent heating and vortexing was required to dissolve Cisplatin.

**2.6 *In Vitro* Drug Screening**

*Low-Mid throughput*: Organoids were cultured for approximately 1-2 weeks and later digested into single cells as described previously. 8,000 cells were seeded in a Matrigel matrix per well of a 96 well plate and left for 10 minutes at 37° $CO_2$, before adding complete gastric organoid media. Cells were left to develop into organoids for 3-4 days. The Tecan D300e Digital Dispenser was used for performing drug treatments. Plates were loaded and T8T Dispensehead Cassettes (Tecan, 30097370) were used to load drugs of 10mM stock concentrations. Drug screen protocols were programmed to dispense drugs at concentrations between 10μM and 0.0007μM in triplicate. DMSO treatment was used as a control, calculated as the highest volume of DMSO used (from the 10μM condition). Organoids were incubated for 3-4 days in the 37° $CO_2$ incubator. Following treatment, cell viability was measured using Cell Titer Blue (Promega, G8081) and the Varioskan Lux from Thermo scientific was used to read plates. Dose response curves were generated and $IC_{50}$ concentrations were calculated using GraphPad PRISM.

*Mid-High throughput*: Cells embedded in Matrigel were seeded into White 384 well plates using a Multidrop Combi Reagent Dispenser by Thermo Scientific. Cells were allowed to develop into organoids for 3 days prior to drug treatments which were performed using an Echo 555 acoustic dispenser by Labcyte using 10 differing concentrations in triplicate. Cells were treated for 1 week before undergoing cell viability analysis. Media was aspirated to the 35μL mark using the 405 Touch Microplate Washer by BioTek and replaced with 25μL of Cell Titer Glo 3D (Promega, G9681) using the Multidrop Combi Reagent Dispenser. Plates underwent 5 minutes of shaking and were then incubated for 30 minutes at room temperature. Luminescence readings were performed using the Synergy Neo HTS reader by BioTek. Dose response curves

and $IC_{50}$ concentrations were generated by XLfit from IDBS using the 4 Parameter Logistic Model.

**2.7 Histology**

To prepare tissue blocks of organoids for further immunohistochemical analysis, 20,000 single cells were seeded into 4-well chambered cell culture slides (Corning, 354114), whereby single cells mixed with Matrigel were first added to each well in a droplet and following solidification gastric organoid media was added. Organoids were maintained until fully developed. For fixing the organoid, chamber slide wells were washed with PBS (400µL) twice. PBS was replaced with 800µL of 4% PFA and left for fixation for at least 2 hours. PFA solution was replaced with diluted Hematoxylin solution (Sigma, HHS32-1L) for 10 minutes followed by 3 washes with $ddH_2O$. 150µL of Histogel (ThermoFisher, HG-4000-012) was added to a Cryomold (Tissue-Trek, 4565) on ice and given time to solidify. Matrigel and cells were added to the cryomold and another 150µL of histogel was added on top. Once solidified, histogel was stored in a tissue cassette and placed in 10% formalin (Sigma Aldrich, HT501128) for 24 hours to allow for histogel fixation. The tissue cassette was then transferred to 70% ethanol and stored until processing.

**2.8 Primary and Secondary Antibodies**

Primary antibodies were diluted in Rockland blocking buffer (Rockland, MB-070) and stored at 4°C. Primary antibodies used include: pERK1/2 (cell signalling 9101L, 1/1000 dilution), ERK1/2 (cell signalling 9107S, 1/1000 dilution), pmTOR (cell signalling 5536P, 1/1000 dilution), ARID1A (Sigma HPA005456, 1/500 dilution), pSTAT3 (cell signalling 9145L,

1/2000 dilution), STAT3 (cell signalling 8768, 1/1000 dilution), pEGFR (cell signalling 2234, 1/1000 dilution), EGFR (cell signalling 2232L, 1/1000 dilution). β-actin was used as a loading control (Sigma, A5441, 1/4000 dilution). HRP-conjugated secondary antibodies were used for detection. For mouse-derived primary antibodies, ECL Peroxidase labelled anti-mouse antibody (NA931VS, 387950) was used. For rabbit-derived primary antibodies, anti-rabbit HRP-linked antibody (cell signalling, 7074S) was used. All secondary antibodies were diluted 1/10,000 in TBS-T. All antibodies were generously provided by Dr. Morag Park.

**2.9 Western Blots**

Flash frozen PDXs were used to generate protein lysates. Tissue samples were minced in a mortar and pestle and added to 300μL of pre-made RIPA solution and phenylmethylsulfonyl (PMSF). Mixture was centrifuged at 10,000 rpm for 10 minutes and the supernatant was used as this has the tissues proteins. Total protein concentration for each protein lysate was measured using a Bradford assay. 200μL of Bio-Rad Protein Assay Dye Reagent Concentrate (BioRad, 5000006) was added to 800μL $dH_2O$ with 2μL of protein to VersaFluor cuvettes (BioRad, 170-2415). A spectrophotometer was used to measure the absorbance at 595nm wavelength. Using a BSA standard curve, the protein concentration was determined based on the absorbance measurements. 30μg of protein lysate was mixed with 5μL of 5X laemlli buffer and completed to 25μL with RIPA lysis buffer. Samples were boiled at 100°C for 5 minutes on a heat block and then centrifuged for 5 minutes at 10,000rpm. NuPAGE 4-12% Bis-Tris pre-cast gels (Invitrogen, NP0336BOX) and MES SDS running buffer (Novex, 2062912) were used for running the gel. Precision Plus Dual Color was used as the protein ladder. Samples were subjected to SDS-PAGE for 1.5 hours at 100V. The gel was then transferred to an Immobilon PVDF nitrocellulose

membrane (Millipore, R9EA35581) at a voltage of 100V for 1.5 hours. Following the transfer, membranes were blocked with diluted Intercept Blocking Buffer, diluted 50% with PBS (Licor, 927-70001) to prevent non-specific binding. Primary antibody solutions were added to membranes and left rocking overnight at 4°C. Membranes were washed with TBS-T (1M Tris pH 8.0, EDTA, 10% tween-20, 5M NaCl) 3 times for 15 minutes and replaced with HRP-conjugated secondary antibody solution for 1 hour, rocking in the dark. Membranes were washed 4 times at 5 minutes intervals with TBS-T. Membranes were imaged using ChemiDoc Luminescence, where membranes were first submerged in a 1:1 mixture of Western Lighting Plus ECL Oxidizing Reagent (PerkinElmer, 265-1840) and Enhanced Luminol Reagent (PerkinElmer, 275-18401). Membrane bands were quantified using ImageJ, whereby phosphorylated protein levels (ie. pERK) were normalized to total levels (ie. ERK) to identify relative levels of protein activation. Membranes were also stripped using NewBlot PVDF Stripping buffer (Licor, 928-40032) to subsequently analyze other primary antibodies.

# CHAPTER 3: RESULTS

## 3.1 Using organoids and PDXs to recapitulate the heterogeneity of the primary tumor

As discussed previously, EGC presents a difficult clinical challenge and is associated with poor prognosis and high mortality rates. Clinical parameters (age, sex, clinical stage at time of diagnosis, treatment intervention and response, and recurrence rates) of 33 EGA patients that underwent surgery at the Montreal General Hospital in Montreal, QC, Canada, were analyzed (**Figure 3A**). PDXs from these patients were sequenced using a 234-gene panel in collaboration with Dr. Adam Bass at Harvard University. The median age of patients at time of diagnosis was 68, with 61% of them being female. 75% of patients were diagnosed at later stage disease (stage III or IV), which as mentioned earlier, is due to the limited number of symptoms at early stage disease. 76% of patients underwent neoadjuvant therapy, although only 21% of those patients elicited a moderate or good response to treatment. 46% of the observed patients demonstrated recurrence of the disease, all of which were distant metastases, such as to the liver, lungs or brain.

Primary tumor tissue was implanted into NSG mice to generate PDXs. Growth rates were determined based on change in tumor volume over time. **Figure 3B** highlights the growth rates for two PDXs, GP201435 and GP201465, whereby both reached sufficient size for collection (~300$mm^3$) by 35 and 45 days respectively. Figure 3B also features the number of days required to achieve a final volume of 300$mm^3$ for 13 other PDX lines. Our PDX cohort displayed a variable growth rate with an average of 84 days to reach end point. Histological analysis was performed on both primary tumor sections and PDX tumor sections to illustrate the conservation of tumor architecture even after mouse implantation (**Figure 3C**). Both GP201435 and

GP201465 tumor sections from primary tumor and PDX are illustrated in Figure 3C, demonstrating the maintenance of the adenocarcinoma from primary tumor to PDX. PDX tumors were also used to derive organoids as highlighted in the Chapter 2 (Materials and Methods). **Figure 3D** displays images captured on the EVOS7000, of organoids from the GP201435 and GP201465 PDX lines. Unlike organoids derived from primary patient material, PDX-derived organoids consist of solely tumor cells, but nonetheless represent the genetic landscape of the original tumor[129].

**A**

| Demographics | N (33) | % |
|---|---|---|
| **Age** | | |
| Median Age (range) | 68 (27-87) | |
| **Sex** | | |
| Female | 20 | 61 |
| Male | 13 | 39 |
| **Clinical Stage** | | |
| I-II | 8 | 25 |
| III-IV | 24 | 75 |
| **Treatment** | | |
| Neoadjuvant | 8 | 24 |
| No Treatment | 25 | 76 |
| **Response to Neoadjuvant** | | |
| Moderate/Good | 7 | 21 |
| Poor | 26 | 79 |
| **Recurrence** | | |
| Distant/Regional | 15 | 46 |
| None | 18 | 54 |

**B**

| | GP201435 | GP201436 | GP201442 | GP201446 | GP201452 | GP201465 | GP201571 | GP201585 | GP2015105 | GP2015108 | GP2015118 | GP2015119 | GP2015121 | G1587474 | G1655928 |
|---|---|---|---|---|---|---|---|---|---|---|---|---|---|---|---|
| Days until 300mm$^3$ | 35 | 33 | 55 | 33 | 40 | 45 | 140 | 92 | 82 | 250 | 61 | 135 | 110 | 98 | 61 |

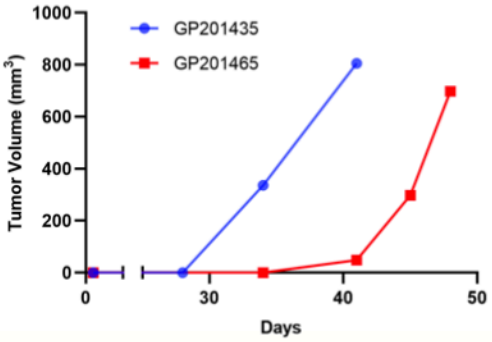


**C**

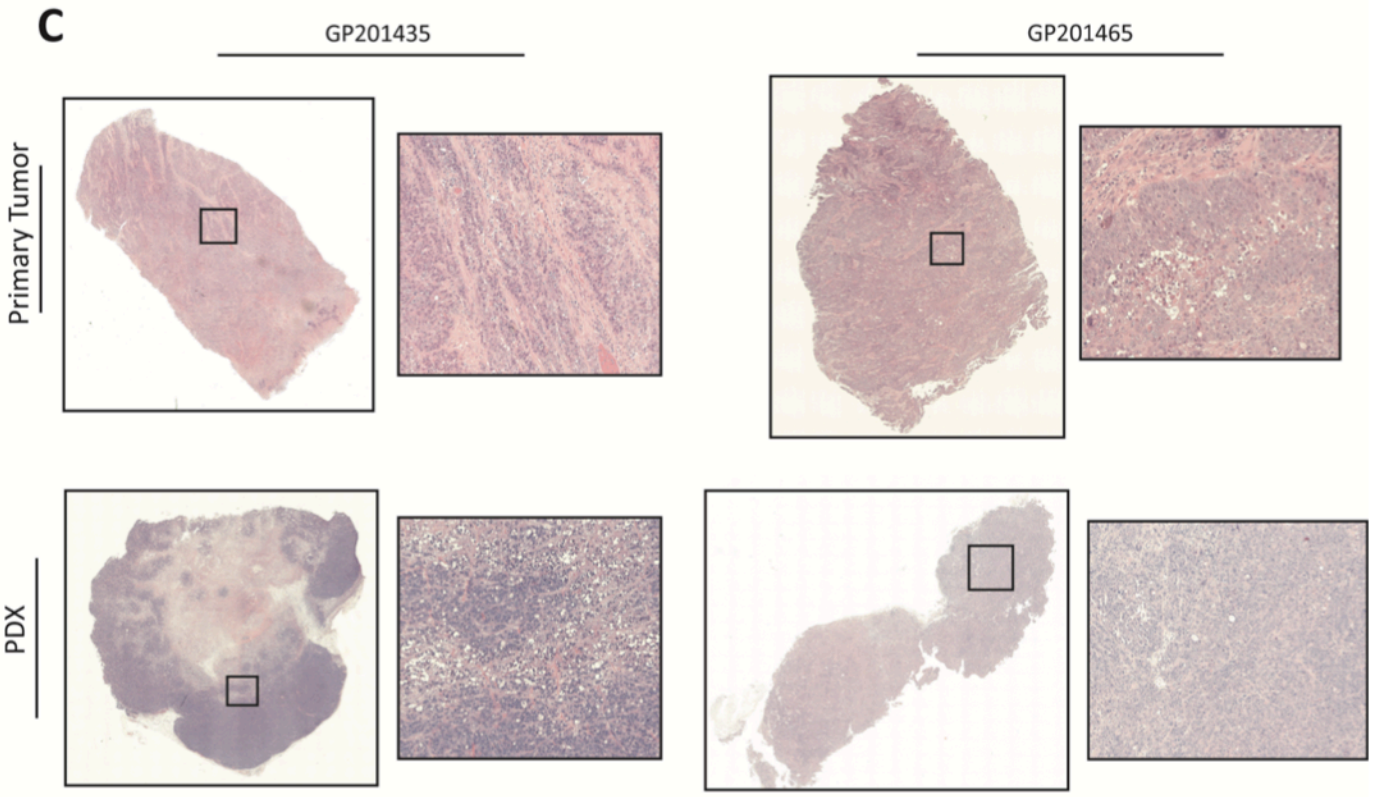


**D**

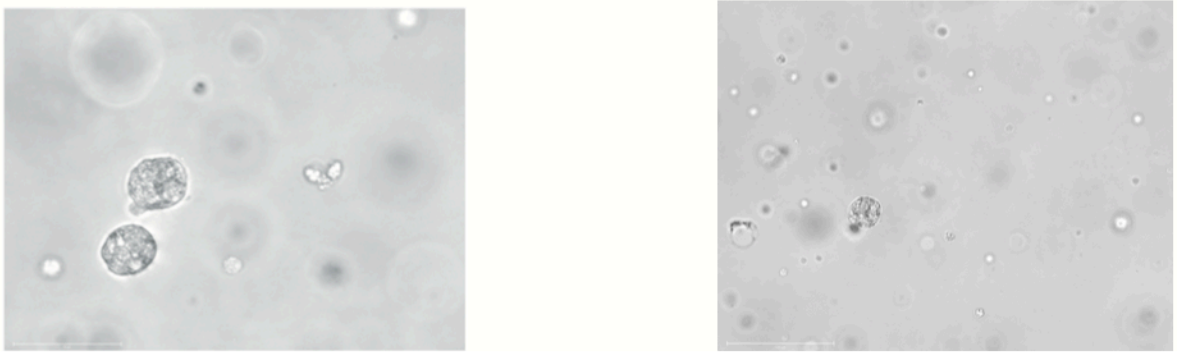

**Figure 3: PDX-derived organoids maintain an adenocarcinoma phenotype**

(A) 33 EGA patients from the Montreal General Hospital were analyzed for clinical parameters such as age, sex, clinical stage at time of diagnosis, treatment intervention and response, and recurrence. All data was gathered on OACIS. (B) Table displays 15 PDX growth curves with ID and number of days to achieve a volume of 300$mm^3$. PDX growth curves for two PDX lines, GP201435 (blue) and GP201465 (red) are shown, plotted as change in tumor volume ($mm^3$) vs. time. (C) Histological sections from Primary Tumor (top) and PDX (bottom) are shown for two gastric adenocarcinoma patients, GP201435 (left) and GP201465 (right). (D) 20X magnification images of organoids from GP201435 (left, size bar = 150μm) and 10X magnification images of organoids from GP201465 (right, size bar = 275μm) taken on the EVOS7000 microscope.

### 3.2 EGAs display a high frequency of alterations in ARID1A and activating mutations of the PI3K/MAPK pathways

33 EGA PDXs were sent for next generation sequencing (NGS) and analyzed for copy number variations (CNVs) and single nucleotide polymorphisms (SNPs) using a gene panel of 234 genes commonly affected in gastric and esophageal cancers. ARID1A mutations were present in 45% of EGA tumors (15/33), marking ARID1A as a potential gene of interest for studying synthetic lethal relationships. **Figure 4A** illustrates the 15 ARID1A-mutant tumors identifying commonly co-occurring genetic mutations, many of which affect the PI3K and MAPK pathways (**Figure 1**). Common alterations of the PI3K pathway included mutations in AKT2 (13%), AKT3 (40%), MDM2 (27%), RICTOR (40%), RPTOR (33%), PIK3CA (40%), PIK3CG (60%), PTEN (33%), ERBB3 (33%) and EGFR (67%). Common alterations of the MAPK pathway included BRAF (60%), KRAS (40%) and MAPK isoforms (73%).

Western blot analysis was performed on PDX tissue protein lysates to match the sequencing data to the protein expression levels in the PDX. **Figure 4B** confirms the lack of ARID1A expression in PDXs with loss or singe base pair mutations of ARID1A. ARID1A is a tumor suppressor acting in the SWI/SNF chromatin remodeling complex and has been previously reported to be mutated in a large subset of cancer types. RMG1, an ovarian cancer cell line known to express ARID1A was used as a positive control. When quantified, the relative levels of ARID1A expression compared to the positive control cell line, are greatly reduced, if not absent altogether, in the ARID1A-mutant PDXs. **Figure 4C** demonstrates the relative activation levels of EGFR in the 15 ARID1A-mutant tumors. A 2-fold increase in pEGFR expression over total EGFR expression is arbitrarily chosen as being ‘activated.’ Even though EGFR showed copy number gain in 10/15 (67%) tumors, EGFR ‘activation’ failed to match the sequencing data. This

does not consider the effects that an EGFR copy number gain may have downstream in the pathways its activating, such as eliciting ERK activation. **Figure 4D** demonstrates the relative activation levels of ERK, a downstream component in the MAPK pathway. Nearly all (12/15) tumors showed some levels of ERK activation (> 2-fold), highlighting the important role ERK has in cancer progression. Since ERK is downstream in the pathway, any upstream mutations or activations have the ability to affect ERK, making ERK a valuable target for halting cancer progression.

**A**

| Genomic Alterations | | Patient | | | | | | | | | | | | | | |
|---|---|---|---|---|---|---|---|---|---|---|---|---|---|---|---|---|
| | | 1 | 2 | 3 | 4 | 5 | 6 | 7 | 8 | 9 | 10 | 11 | 12 | 13 | 14 | 15 |
| ARID1A | *100%* | Y | Y | Y | Y | Y | Y | Y | Y | Y | Y | Y | Y | Y | Y | Y |
| ARID1B | *40%* | Y | | | Y | | Y | | | | Y | | Y | | Y | |
| EGFR | *67%* | Y | | | | | Y | | Y | Y | Y | Y | Y | Y | Y | Y |
| ERBB2 | *13%* | | Y | | Y | | | | | | | | | | | |
| ERBB3 | *33%* | Y | | | | | Y | Y | | | | | Y | | Y | |
| BRAF | *60%* | Y | | | | | Y | Y | Y | Y | Y | Y | Y | | | Y |
| KRAS | *40%* | | | | | | Y | Y | Y | Y | | Y | | | | Y |
| PIK3CA | *40%* | | | | Y | Y | | Y | | | Y | | Y | | Y | |
| PIK3CG | *60%* | Y | | | Y | Y | Y | | Y | | Y | Y | Y | | | Y |
| PTEN | *33%* | | | | | | | | Y | Y | | Y | Y | | Y | |
| AKT2 | *13%* | | | | | | | | Y | | Y | | | | | |
| AKT3 | *40%* | Y | | | | Y | | | Y | | | Y | Y | | Y | |
| RICTOR | *40%* | | Y | | | Y | | | | Y | | Y | | | Y | Y |
| RPTOR | *33%* | Y | | | | | Y | | Y | Y | | | | Y | | |
| MDM2 | *27%* | | | | | | Y | Y | Y | | | | | | Y | |
| SMARCA4 | *33%* | Y | | | | | | Y | Y | | | Y | | | | Y |
| SMARCA5 | *33%* | | | | | | | | Y | | | Y | Y | | Y | Y |

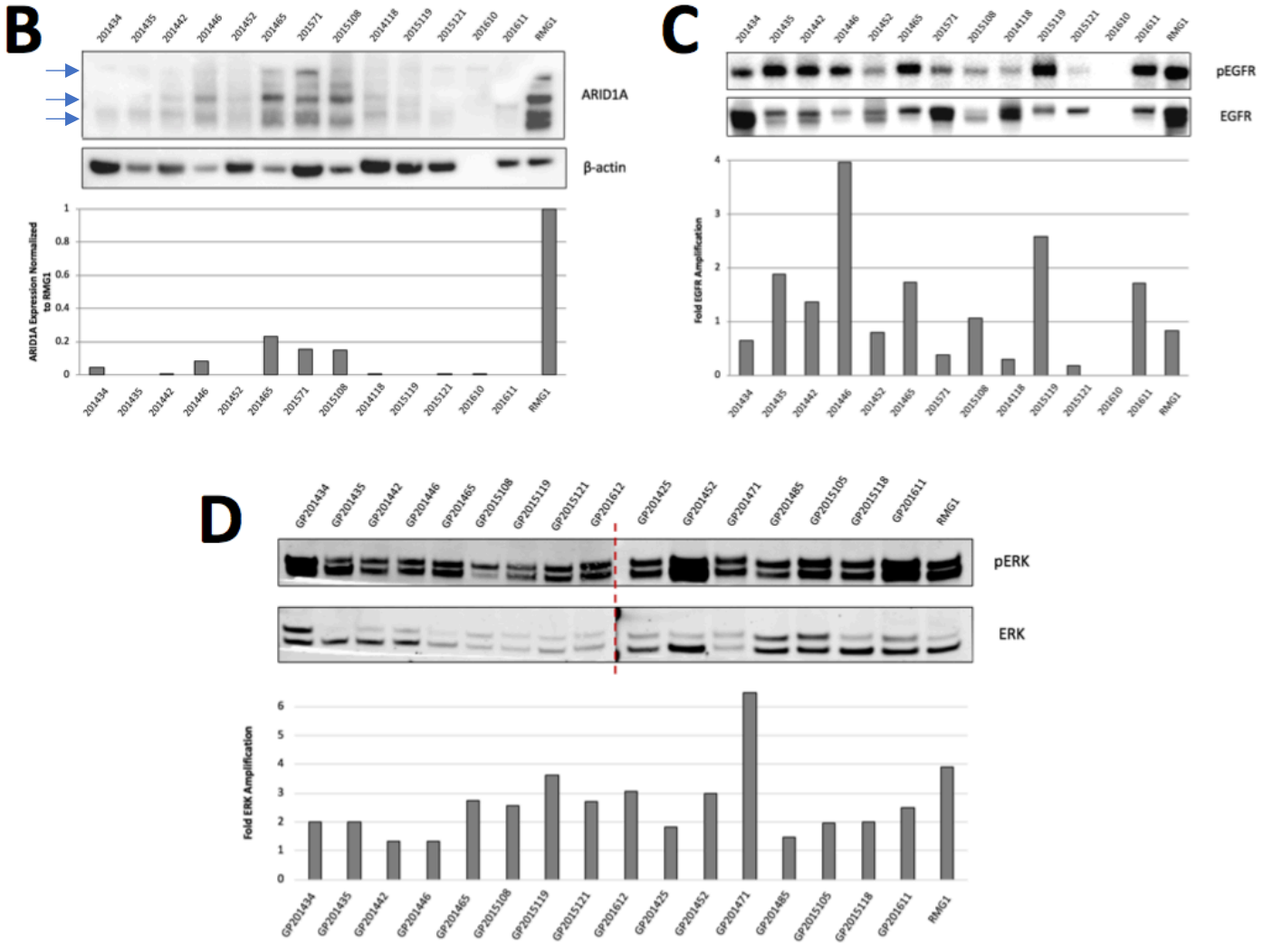

**Figure 4: ARID1A-mutant EGAs exhibit high frequency of co-occurring alterations in the PI3K/MAPK pathways**

(A) 33 EGA PDXs were sent for NGS and analyzed for CNVs and SNPs. Sequencing was performed using a gene panel of 234 genes commonly altered in EGC in collaboration with Adam Bass from Harvard University. 15 PDXs with ARID1A loss or mutations are shown, and co-occurring genetic alterations are listed including ARID1B, AKT2, AKT3, BRAF, KRAS, MDM2, RICTOR, RPTOR, PIK3CA, PIK3CG, PTEN, ERBB3, EGFR, SMARCA4 and SMARCA5. Alteration frequency is listed on the left. 'Y' indicates either a copy number gain, copy number loss, missense mutation, nonsense mutation or frameshift mutation. 3' UTR mutations are not shown. (B) PDX protein lysates were used to identify ARID1A protein expression levels in ARID1A-mutant tumors. RMG1 was used a positive control cell line for ARID1A expression. β-actin was used as a loading control. Signals were quantified using Image J. ARID1A signals were normalized to β-actin signals, and then normalized to RMG1 expression levels. Blue arrows indicate the three bands used to quantify ARID1A expression (different isoforms yield products at ~250kDa, 170kDa and 150kDa). (C) Protein lysates from (B) were used to identify relative levels of EGFR expression. pEGFR (anti-rabbit) and total EGFR (anti-mouse) were immunoblotted on the same membrane and signals were separated using different secondary antibodies. Signals were quantified using ImageJ. Fold EGFR amplification represents pEGFR levels normalized to total EGFR levels. (D) Western blot analysis of pERK and total ERK was performed and quantified in a similar manner as (C). Two membranes were used and were merged at the dotted line in the figure. In order to match sequencing data to western blot data, the matched Patient ID to PDX ID is as follows: Patients 1 (201434), 2 (201435), 3

(201436), 4 (201442), 5 (201446), 6 (201452), 7 (201465), 8 (201571), 9 (2015108), 10 (2015118), 11 (2015119), 12 (2015121), 13 (201610), 14 (201611), 15 (201585)

### 3.3 EGAs show increased sensitivity to MAPK targeted therapies

After identifying PI3K and MAPK pathway related genes to be commonly affected in EGA, we wanted to perform high-throughput drug screens on PDX-derived organoids using drugs targeting those pathways. Two PDX-derived organoid lines were tested in our screen: GP201435 and GP201465. Twelve drugs were tested including an EZH2 inhibitor *UNC1999*, EGFR inhibitor *Gefitinib*, ERK inhibitor *Ulixertinib*, a dual PIK3CA/mTOR inhibitor *Gedatolisib*, MEK inhibitor *Trametinib*, MET inhibitor *Crizotinib*, VEGFR inhibitor *Sorafenib*, HSP90 inhibitor *Luminespib*, BRAF inhibitor *Dabrafenib*, PIK3CG inhibitor *Duvelisib*, mTOR inhibitor *Sirolimus* and AKT inhibitor *Uprosertib*.

GP201435 harbors ARID1A loss with MAP3K5 and mTOR complex amplifications. **Figure 5A** highlights the results of the GP201435 drug screen. This organoid line was most sensitive to the HSP90 inhibitor Luminespib and the MEK inhibitor Trametinib with $IC_{50}$ concentrations of 9nM and 2nM respectively. They also showed sensitivity to Gefitinib and Ulixertinib with $IC_{50}$ concentrations of 10nM and 0.1μM respectively. This line was not sensitive to the mTOR inhibitor Sirolimus, which was predicted by the mTOR complex mutation, although was sensitive to the dual PIK3CA/mTOR inhibitor Gedatolisib with an $IC_{50}$ concentration of 0.27μM.

GP201465 also has ARID1A loss as well as MAP3K8 loss, with BRAF and KRAS amplifications, and a missense mutation in PIK3CA. **Figure 5B** highlights the results of the GP201465 drug screen. This organoid line was most sensitive to the ERK inhibitor Ulixertinib and the MEK inhibitor Trametinib with $IC_{50}$ concentrations of 0.1μM and 0.015μM. The line was resistant to all other drugs, including BRAF inhibitor Dabrafenib and EGFR inhibitor Gefitinib. Mutations in MAP3K8 have been shown to activate the MAPK pathway independent of EGFR

and other RTKs, activating it downstream at the level of MEK. This could explain why ERK activation is still noticeable and drugs other than MEK and ERK inhibitors failed to elicit a response. Based on our high-throughput drug screening results, we decided to shift our focus to targeting the MAPK pathway, with special attention for Ulixertinib and Trametinib, which have yet to be explored in EGA.

**A**

| Drug | Target | IC50 (μM) |
|---|---|---|
| UNC1999 | EZH2 | 11 |
| Gefitinib | EGFR | 0.01 |
| Ulixertinib | ERK1/2 | 0.1 |
| Gedatolisib | PIK3CA/mTOR | 0.27 |
| Trametinib | MEK | 0.002 |
| Crizotinib | MET | 3 |
| Sorafenib | VEGFR | 2.5 |
| Luminespib | HSP90 | 0.009 |
| Dabrafenib | BRAF | 25 |
| Duvelisib | PIK3CG | 37 |
| Sirolimus | mTOR | 21 |
| Uprosertib | AKT/1/2/3 | 18.3 |

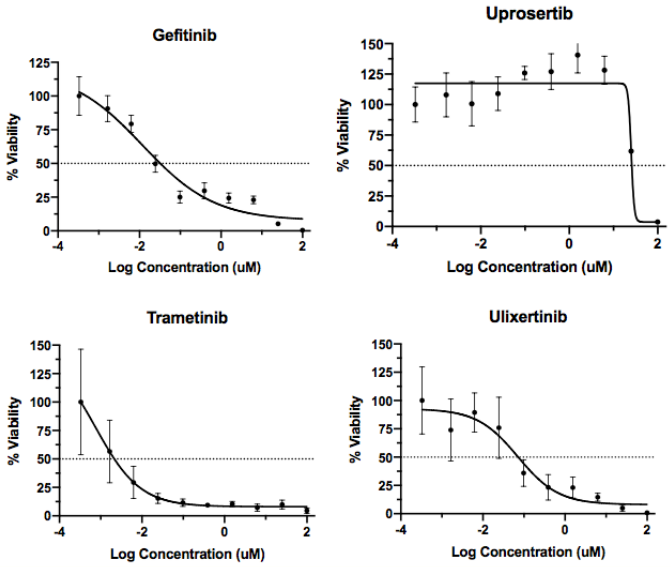


**B**

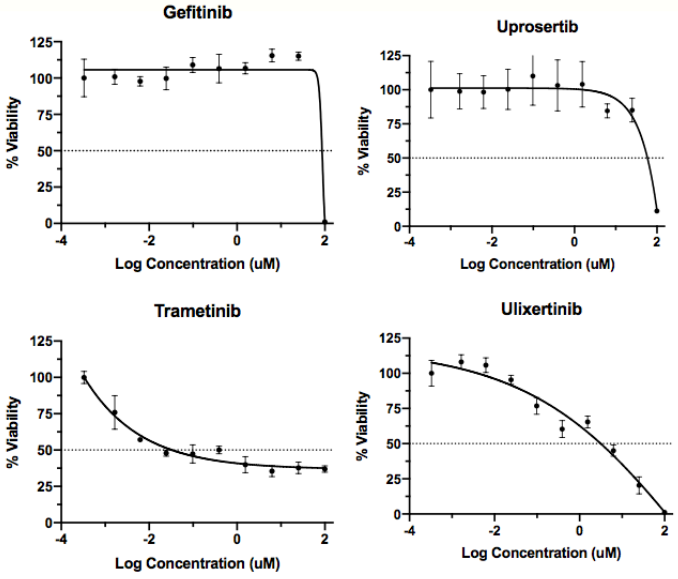


| Drug | Target | IC50 (μM) |
|---|---|---|
| UNC1999 | EZH2 | 20 |
| Gefitinib | EGFR | 88 |
| Ulixertinib | ERK1/2 | 0.1 |
| Gedatolisib | PIK3CA/mTOR | 3 |
| Trametinib | MEK | 0.015 |
| Crizotinib | MET | 37 |
| Sorafenib | VEGFR | 4 |
| Luminespib | HSP90 | 4.3 |
| Dabrafenib | BRAF | 18.9 |
| Duvelisib | PIK3CG | 27.8 |
| Sirolimus | mTOR | 15.3 |
| Uprosertib | AKT/1/2/3 | 84 |

**Figure 5: EGAs display sensitivity to the MAPK targeting drugs Trametinib and Ulixertinib**

PDX-derived organoids were used to perform high-throughput drug screens using 12 drugs (target in brackets): UNC1999 (EZH2), Gefitinib (EGFR), Ulixertinib (ERK), Gedatolisib (PIK3CA/mTOR), Trametinib (MEK), Crizotinib (MET), Sorafenib (VEGFR), Luminespib (HSP90), Dabrafenib (BRAF), Duvelisib (PIK3CG), Sirolimus (mTOR) and Uprosertib (AKT). 2 PDX-derived organoid lines were tested: GP201435 (A) and GP201465 (B). Organoids were plated in 384 plates and left to grow for 3 days. Drugs were given at 10 concentrations in triplicate and cells were incubated for 1 week. Cell viability was measured using Cell Titer Glow. Dose response curves were generated using GraphPad PRISM and $IC_{50}$ concentrations were generated. Four representative dose response curves are displayed for each line: Gefitinib, Uprosertib, Ulixertinib and Trametinib. Dose response curves are plotted as the Logarithmic concentration in μM versus the % of cells alive compared to DMSO control. Summary table displays the drug name, its target and the calculated $IC_{50}$ concentration in μM. Red indicates resistance, blue indicates sensitivity.

### 3.4 Trametinib and Ulixertinib suggest eliciting non-specific responses independent of ARID1A alterations

In order to identify whether the success of Trametinib and Ulixertinib at reducing cell viability in the two EGAs tested was attributed to on-target effects, other MEK and ERK inhibitors were investigated. **Figure 6A** highlights that no clear relationship is observed between ARID1A and Trametinib/Ulixertinib responses. 14/15 of the organoid lines showed an $IC_{50}$ concentration of 0.1μM or less, including the 2 WT ARID1A organoid lines, signifying the Trametinib response is more likely due to toxicity. Furthermore, the 8 organoid lines tested with Ulixertinib showed varying $IC_{50}$ concentrations stretching over a 10-fold concentration range (0.1-2μM). Although only 3 of these lines had a confirmed ARID1A mutation, further investigation is required to identify the mutational profiles of the remaining 5 lines. Nonetheless, the differences in response to Ulixertinib would remain modest.

The GP201435 organoid line was tested for 3 additional MEK inhibitors; Binimetinib, Selumetinib and U0126 and 3 additional ERK inhibitors; FR180204, SCH772984 and LY3214996. **Figure 6B** highlights the results of the drug screen. Although this organoid line was sensitive to Trametinib and Ulixertinib with $IC_{50}$ concentrations of 0.002μM and 0.1μM respectively, it was resistant to all other MEK and ERK inhibitors, with consistent $IC_{50}$ concentrations ranging from 11-16μM. Although Trametinib has been established as a more potent MEK inhibitor, most studies only identify a roughly 10-fold increase in potency[130]. This cannot explain the significantly lower $IC_{50}$ concentration observed in the drug screen. Other studies have identified very similar kinetics and potency among the four ERK inhibitors[131]. These results suggest Trametinib and Ulixertinib act through enhanced toxicity and off-target effects.

Further investigation was conducted to establish whether EGAs with ARID1A alterations would respond better to Trametinib and Ulixertinib. 15 organoid lines were tested for Trametinib, while only 8 of them were simultaneously tested for Ulixertinib. Of the 15 organoid lines, 8 showed an ARID1A alteration with ARID1A loss confirmed through protein expression levels (**Figure 4B**), 2 organoid lines were wild type for ARID1A, also confirming ARID1A protein expression through western blot analysis, while 5 organoid lines had an unknown ARID1A mutational profile.

**A**

| Patient | ARID1A mutation? | Trametinib IC50 (μM) | Ulixertinib IC50 (μM) |
|---|---|---|---|
| 1 | Y | 0.002 | 0.1 |
| 2 | Y | 0.015 | 0.1 |
| 3 | Y | 0.019 | 0.33 |
| 6 | Y | 1.6 | N/A |
| 8 | Y | 0.13 | N/A |
| 10 | Y | 0.03 | N/A |
| 14 | Y | 0.3 | N/A |
| 15 | Y | 0.04 | N/A |
| 16 | N | 0.01 | N/A |
| 17 | N | 0.05 | N/A |
| 18 | Unknown | 0.07 | 2 |
| 19 | Unknown | 0.0046 | 0.67 |
| 20 | Unknown | 0.018 | 1 |
| 21 | Unknown | 0.07 | 1.4 |
| 22 | Unknown | 0.03 | 0.8 |

**B**

| Target | Drug | IC50 (μM) |
|---|---|---|
| MEK | Trametinib | 0.002 |
| | Binimetinib | 16 |
| | Selumetinib | 13 |
| | U0126 | 11 |
| ERK | Ulixertinib | 0.1 |
| | FR180204 | 16 |
| | SCH772984 | 15 |
| | LY3214996 | 15 |

**Figure 6: Organoid response to Trametinib and Ulixertinib do not correlate with ARID1A status and most likely act through off-target effects**

(A) 10 PDX-derived organoid lines (1, 2, 3, 6, 10, 14-17) and 5 primary organoid lines (18-22) were tested for response to Trametinib and Ulixertinib. The 10 PDX-derived organoid lines were tested for ARID1A alterations (Y) or WT ARID1A (N). Organoids were plated in 96-well plates and left to grow for 3 days. Drugs were delivered at 10 concentrations in triplicate and cells were incubated for 3 days. Cell viability was measured using Cell Titer Blue. Dose response curves were generated using GraphPad PRISM and $IC_{50}$ concentrations (in μM) were generated and summarized in the table. (B) The PDX-derived organoid line GP201435 was used to perform a drug screen using the following 8 drugs (target in brackets): Trametinib (MEK), Binimetinib (MEK), Selumetinib (MEK), U0126 (MEK), Ulixertinib (ERK), FR180204 (ERK), SCH772984 (ERK) and LY3214996 (ERK). The $IC_{50}$ concentrations (in μM) are displayed in the table, with blue indicating sensitivity and red indicating resistance to treatment.

### 3.5 Targeting the PI3K pathway remains a viable option for treating ARID1A-mutant EGAs

Although targeting the MAPK pathway was deemed to be not significant due to the evident off-target effects of Trametinib and Ulixertinib, targeting the PI3K pathway remains a viable alternative. **Figure 7B** shows the MAPK and PI3K pathway components with respective inhibitors used to target them. The dual PIK3CA and mTOR inhibitor Gedatolisib was investigated in 9 PDX-derived organoid lines, 7 of which are ARID1A-mutant. **Figure 7A** highlights the response of each line to Gedatolisib, while comparing their mutational profiles. When comparing drug response to solely ARID1A mutation, there is no evident correlation as the $IC_{50}$ concentrations vary. Although, ARID1A-mutant organoid lines with PI3K alterations and RICTOR mutations, a component of the mTORC2 complex, showed increased sensitivity to Gedatolisib, as shown with patients 14 and 15 ($IC_{50}$ concentrations of 0.08μM and 0.06μM respectively). Notably, patient 16 with a PIK3CA and RICTOR mutation, but no ARID1A alteration was resistant to Gedatolisib. Other organoid lines with ARID1A loss and either a PI3K or mTOR complex alteration showed less success with Gedatolisib. Patients 6 and 8 showed ARID1A loss with PI3K and RPTOR alterations although showed little efficacy with the drug. Therefore, patients with specified genetic profiles including ARID1A loss and PI3K and RICTOR mutations may benefit from Gedatolisib, although further investigation is required.

**A**

| Patient | Gedatolisib IC50 (μM) | ARID1A mutation | PIK3CA mutation | PIK3CG mutation | RICTOR mutation | RPTOR mutation | BRAF mutation | KRAS mutation |
|---|---|---|---|---|---|---|---|---|
| 2 | 0.18 | Y | | | Y | | | |
| 6 | 2.8 | Y | | Y | | Y | Y | Y |
| 7 | 3 | Y | Y | | | | Y | Y |
| 8 | 1.9 | Y | | Y | | Y | Y | Y |
| 10 | 0.27 | Y | Y | Y | | | Y | |
| 14 | 0.08 | Y | Y | | Y | | | |
| 15 | 0.06 | Y | | Y | Y | | Y | Y |
| 16 | 17.9 | | Y | | Y | | | Y |
| 17 | 0.27 | | | Y | | | | |

**B**

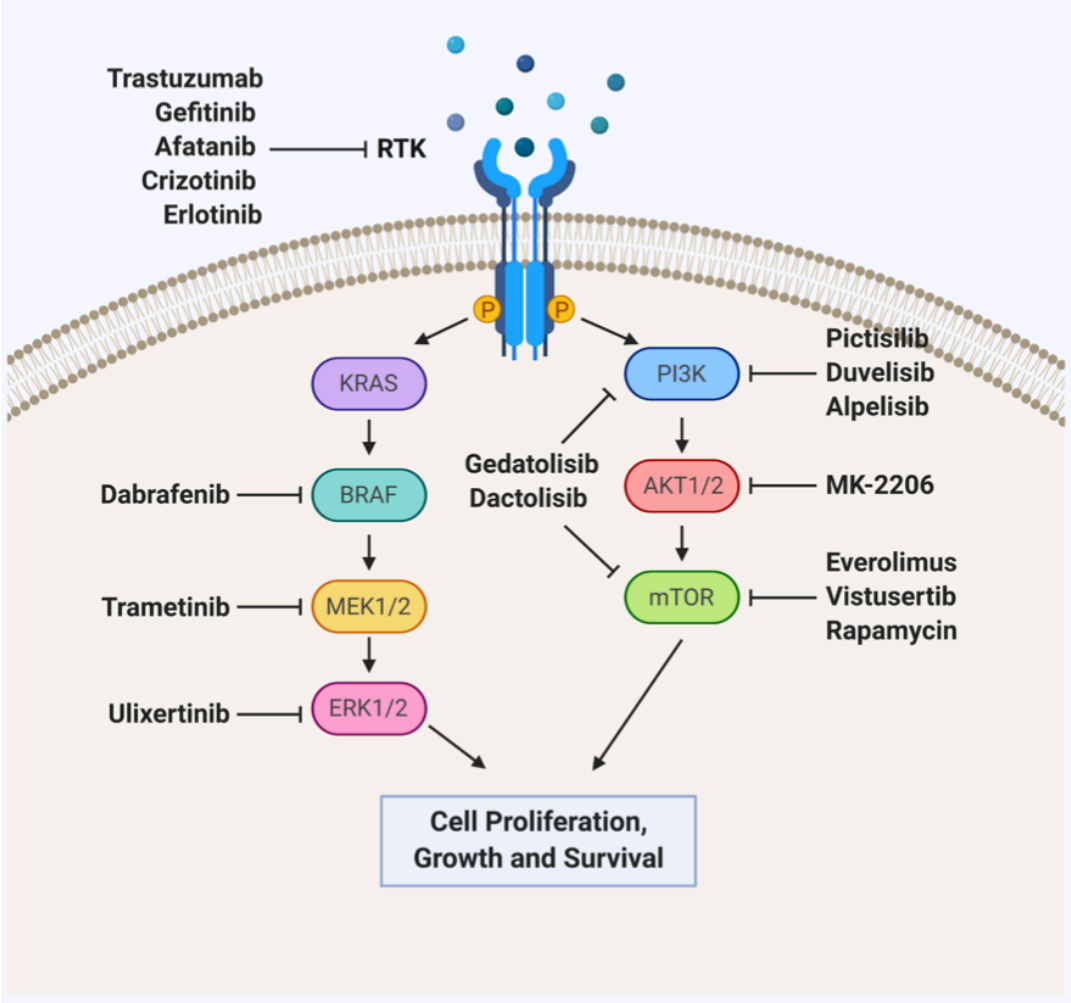

**Figure 7: ARID1A-mutant EGAs with PI3K and RICTOR mutations show good response to Gedatolisib**

(A) 9 PDX-derived organoid lines were treated with Gedatolisib in a similar manner to previous high-throughput drug screens and $IC_{50}$ concentrations were determined through dose response curves. Summary table highlights the $IC_{50}$ concentration (in μM), where blue indicates a sensitive organoid line, and red indicates a resistant organoid line. Following columns summarize the mutational profiles of ARID1A, PIK3CA, PIK3CG, RICTOR, RPTOR, BRAF and KRAS, where a 'Y' indicates a genomic alteration is present. (B) Schematic of the MAPK pathway (left) and the PI3K pathway (right), with respective drugs that target their components.

# CHAPTER 4: DISCUSSION & CONCLUSION

Gastric and esophageal cancers have respective five-year survival rates of approximately 25% and 15%, making them some of the deadliest cancers worldwide[3]. Despite having such high mortality rates, gastric cancer research remains underfunded, which has hindered the advancement of novel therapies[132,133]. Current standard of care for patients is the surgical resection of the tumor complemented with perioperative DCF therapy[17]. Although this is presently the most effective chemotherapy regimen available for EGC, it is not immaculate as only 60% of patients initially respond to treatment, with nearly another 50% of those patients developing resistance[22]. The modest response has largely been attributed to genomic inter- and intra-tumor heterogeneity. More recently, we have been moving from the 'one size fits all' approach to treating cancer and entering an era of precision and predictive medicine, often guided by molecular testing. One of the only targeted therapies used in the clinic for treating EGC is Trastuzumab in HER2-amplified tumors[31]. Nonetheless, many patients still progress following first-line Trastuzumab treatment[50]. Angiogenesis inhibitors such as Ramucirumab have shown clinical utility as second-line therapies[47]. No other genomic biomarkers investigated, such as EGFR and MET, have shown success in Phase III clinical trials (Table 1). Many other targeted therapies, including those against the MAPK and PI3K pathways may provide a potential alternative for patients of a definite genomic background. Although there is promise for using PI3K and MAPK pathway inhibitors in other cancer types such as breast and lung cancers, their utility remains largely unknown for EGC[134,135].

In this study, we aimed to investigate the value of MAPK and PI3K pathway targeting drugs in ARID1A-mutant EGAs. Primary patient material was subcutaneously implanted into

mice to form PDXs, which were subsequently utilized to derive organoids. PDXs were sequenced and western blot analysis was performed to compare the genomic data with protein expression levels. Sequencing data showed a high alteration frequency of the tumor suppressor ARID1A, commonly co-occurring with activating mutations of the PI3K and MAPK pathways, comparable to previous reports. ARID1A-mutant PDX-derived organoids were used to perform high-throughput drug screens using a variety of MAPK and PI3K pathway targeting drugs. It was first demonstrated that a number of organoid lines responded well to the MEK inhibitor Trametinib and ERK inhibitor Ulixertinib. Additional screening with other MEK and ERK inhibitors showed reduced sensitivity, suggesting Trametinib and Ulixertinib were acting in non-specific manners. Furthermore, Trametinib responded well in all organoid lines, irrespective of the genomic status of ARID1A. A potential alternative included the dual PI3K/mTOR inhibitor Gedatolisib, which showed higher sensitivity in organoid lines with ARID1A loss and mutations in PI3K and RICTOR. Further investigation is required to study the value of ARID1A as a biomarker for MAPK/PI3K pathway targeting agents.

Sequenced PDXs from 33 EGA patients were analyzed and revealed to have heterogenous mutational profiles. 45% (15/33) of PDXs revealed ARID1A loss (CNV) or mutations (SNP; missense, frameshift or nonsense). Western blot analysis confirmed reduced or lack of ARID1A protein expression in all 15 PDXs (Figure 4B). This high alteration frequency is comparable to other EGC databases. Most notably, The Cancer Genome Atlas (TCGA) Research Network reported alterations of ARID1A in 33% of stomach adenocarcinomas and 15% of esophageal adenocarcinomas[27,28]. Furthermore, our data suggest that ARID1A loss frequently co-occurs with activating mutations of PIK3CA (40%), PIK3CG (60%), RICTOR (40%), RPTOR (33%), EGFR (67%), BRAF (60%) and KRAS (40%). Similar studies have shown co-occurring

alterations of ARID1A with PI3K and MAPK pathway components[103]. ARID1A has been under investigation recently for potential synthetic lethality opportunities, including with the PI3K pathway. Kwan et al. showed that the mTOR inhibitor AZD8055, PI3K inhibitor NVP-BEV235 and AKT inhibitor MK-2206 all showed enhanced sensitivity in ARID1A-mutant cancer cell lines relative to ARID1A WT lines[136]. Other studies showed similar findings, including upregulation of the PI3K and MAPK pathways following ARID1A knockdown, suggesting a critical role for ARID1A in PI3K pathway activation[137]. The mechanism by which ARID1A modulates PI3K pathway activity remains unclear. It has been shown that in ovarian cancer ARID1A inhibits the PI3K pathway via promoting expression of the PI3K suppressor PIK3IP1[138]. Similarly, in breast cancer, ARID1A acts as a negative regulator of ANXA1, which functions to promote AKT phosphorylation[139]. The aim of our study was to use ARID1A loss as a biomarker for investigating sensitivity to PI3K and MAPK pathway targeted therapies.

Western blot analysis was performed to compare sequencing data with the protein expression levels of the PDXs. All ARID1A-mutant PDXs showed reduced or lack of ARID1A expression (Figure 4B). 12/15 ARID1A-mutant PDXs showed ERK activation, indicating hyperactivity of the MAPK pathway (Figure 4D). Notably, EGFR activation did not coincide with the mutational profile of the PDX (Figure 4C). However, this does not consider downstream events in the pathway. Intra-tumor heterogeneity may be one of the reasons for which the sequencing data does not overlap with the protein expression profile. As referred to in Figure 4A, the PDXs studied showed a large number of mutations, all of which included alterations within the MAPK and PI3K pathways. This heterogeneity also acts as the major barrier for finding effective targeted therapies.

*In vitro* drug screening on two PDX-derived organoid lines (GP201435, GP201465) revealed sensitivity to the ERK inhibitor Ulixertinib and MEK inhibitor Trametinib. GP201435 (Figure 5A) contained a number of genomic alterations in addition to ARID1A loss, including ERBB2 amplification and MAP3K5 and RICTOR mutations. It responded well to three additional drugs, Gefitinib (*EGFRi*), Gedatolisib (*PIK3CA/mTORi*) and Luminespib (*HSP90i*). The second line (GP201465 from Figure 5B) showed no additional responses despite having a large number of mutations including in FGFR4, BRAF, KRAS, MAP3K8, PIK3CA and MDM2. Both lines had a number of MAPK alterations and confirmed ERK activation in western blots (Figure 4D). One potential limitation of organoid drug screening is the change in genetic makeup with serial passaging, as the drug screens for the lines studied were done at their 10$^{th}$ passage. Previous studies have alluded to organoids gaining genetic mutations with subsequent passages, which could affect their response to drugs over time. Despite the genetic drift with serial passaging, most studies have shown that significant changes don't begin until at least 16 passages, with only non-cancer driver mutations evident before that[117].

Further drug screening with other MEK and ERK inhibitors suggested Trametinib and Ulixertinib were eliciting off-target effects. We screened the GP201435 organoid line with 3 additional MEK inhibitors (Selumetinib, Binimetinib and U0126) and 3 additional ERK inhibitors (FR180204, SCH772984 and LY3214996) and found the MEK inhibitors were 10,000 times less sensitive than Trametinib, while the other ERK inhibitors were 100 times less sensitive than Ulixertinib (Figure 6A). Previous analyses on Trametinib suggest a similar mechanism of action as Selumetinib and Binimetinib, allosterically binding to MEK1 and preventing RAF-mediated phosphorylation of the S217 residue[130,140]. Although Trametinib has been shown to be more potent and effective at targeting MEK1/2, several studies suggest a

modest 10-fold increase in sensitivity for the same concentration of drug, which cannot explain the 10,000-fold increase in sensitivity observed in our screen[130]. Similarly, Ulixertinib has shown a similar mechanism of action and affinity for ERK1/2 with equivalent kinetics as SCH772984[131]. As these studies on potency were conducted on 2D cell lines, further investigation should be conducted to see whether the increased potency of Trametinib may be attributed to the nature of 3D organoid response. 15 organoid lines were tested for response to Trametinib, 8 of which had ARID1A loss, 2 were ARID1A WT (wild type) and 5 had unknown genetic profiles. 14/15 organoid lines responded well (with $IC_{50}$ concentrations below 0.1μM) to the MEK inhibitor suggesting the Trametinib response was due to toxicity (Figure 6B). Similarly, no clear relationship was observed between the organoid's response to Trametinib and Ulixertinib and their ARID1A mutational status. While ARID1A loss is likely not a biomarker for MEK and ERK targeted therapies, this does not indicate Trametinib wouldn't find success in the clinic. Over the last decade MEK targeted therapies have been under extensive investigation for its critical role in cancer progression. Trametinib is currently used in combination with the BRAF inhibitor dabrafenib in metastatic melanoma patients with a $BRAF^{V600E}$ mutation[85]. There are currently a number of ongoing Phase III clinical trials involving Trametinib for a variety of cancer types, although none for gastric and esophageal cancers[141]. Our results suggest Trametinib may be a suitable candidate for EGC patients with MAPK alterations. Further investigation is required however, such as confirming the sensitivity of Trametinib *in vivo*. Furthermore, tests should be conducted to observe any off-target effects of Trametinib and confirm its effects are not solely due to MEK inhibition.

Our *in vitro* drug screen identified the dual PI3K and mTOR inhibitor Gedatolisib as a potential alternative to MAPK targeted therapies. ARID1A-mutant organoid lines with PI3K and

RICTOR mutations showed enhanced sensitivity to Gedatolisib compared to an ARID1A WT organoid line with a similar genetic profile (Figure 7A). However, ARID1A-mutant organoid lines with PIK3CG and RPTOR mutations showed reduced sensitivity to the inhibitor. The discrepancy in response between RICTOR and RPTOR amplified EGCs may be attributed to the mTOR complexes they reside in. RPTOR functions in the mTORC1 complex, which is activated downstream by AKT and is known to be sensitive to rapamycin[142]. RICTOR is a subunit of the mTORC2 complex, which has a variety of functions, one of which is to act upstream and promote AKT activation[142]. mTORC2 is rapamycin insensitive, which was evident in the GP201435 drug screen (Figure 5A), as this organoid line had a RICTOR mutation but did not respond to the mTOR inhibitor. Several studies have alluded to the critical role RICTOR plays in PI3K pathway activation and how mTORC1 complex inhibition (ie. RPTOR inhibition) often results in drug resistance due to the counter effects of RICTOR[143]. The critical role of RICTOR could account for increased sensitivity of organoid lines with RICTOR amplifications compared to those with RPTOR amplifications. Although ARID1A-mutant organoid lines with both PI3K and RICTOR mutations showed enhanced sensitivity to Gedatolisib, there was no clear relationship between ARID1A loss alone. This suggests the potential for using ARID1A as a synthetic lethal candidate for PI3K pathway targeting agents. Further investigation is required to assess whether ARID1A loss is required to sensitize organoid lines with PI3K and RICTOR mutations to Gedatolisib. This includes testing a larger number of ARID1A WT and ARID1A-mutant EGCs with comparable genomic backgrounds. Gedatolisib is currently showing promise in early phase clinical trials for NSCLC, OCCC, pancreatic cancer and breast cancer[144]. Gedatolisib has yet to be investigated in EGC or in relation to ARID1A expression.

Regardless of the potential for targeted therapies in EGC, the effectiveness of monotherapies remains unclear. A study by Soares, HP et al. found that the dual PI3K/mTOR inhibitor NVP-BEZ235 blocked PI3K pathway activation, while simultaneously activating the MAPK pathway[145]. They highlighted that NVP-BEZ235 acts to block mTORC1-mediated phosphorylation of S6 and 4E-BP1 and mTORC2-mediated phosphorylation of AKT[145]. Although, the RICTOR subunit of mTORC2 which normally acts to mediate a negative feedback loop on MEK activation becomes suppressed in the process, leading to ERK hyperactivation[145]. This study underscores the complexity of the PI3K and MAPK pathways and questions whether a monotherapy such as Gedatolisib would be successful in the clinic. *In vivo* studies should be conducted to identify whether continuous treatment with Gedatolisib would be effective. Similarly, high-throughput combination drug screens on PDX-derived organoid lines should be performed to identify additive or synergistic drug effects.

In conclusion, there is an increasing appreciation for the potential of targeted therapies in EGC. This study aimed to identify MAPK and PI3K pathway targeting agents as potential treatment options in ARID1A-mutant EGCs. Nearly 50% of PDXs from primary patient material were found to express ARID1A alterations, often co-occurring with mutations in the PI3K and MAPK pathways. High-throughput drug screening on two ARID1A-mutant organoid lines identified the MEK inhibitor Trametinib and ERK inhibitor Ulixertinib as potential synthetic lethal candidates. Drug screens with other organoid lines identified no correlation between ARID1A status and drug response. Furthermore, an ARID1A-mutant organoid line responding well to Trametinib and Ulixertinib responded poorly to other MEK and ERK inhibitors, suggesting these drugs work through off-target effects. Gedatolisib, a dual PI3K/mTOR inhibitor remains a viable alternative for ARID1A-mutant EGCs, as organoid lines with ARID1A loss and

PI3K and RICTOR mutations showed greater sensitivity than ARID1A WT lines with similar genetic profiles. Further studies are required to assess the importance of ARID1A loss on drug response, as well as testing combination therapies, such as Gedatolisib with Trametinib or Ulixertinib, to identify synergistic drug effects.

## REFERENCES


1 Rawla, P. & Barsouk, A. Epidemiology of gastric cancer: global trends, risk factors and prevention. *Prz Gastroenterol* **14**, 26-38, doi:10.5114/pg.2018.80001 (2019).

2 Wong, M. C. S. *et al*. Global Incidence and mortality of oesophageal cancer and their correlation with socioeconomic indicators temporal patterns and trends in 41 countries. *Scientific Reports* **8**, 4522, doi:10.1038/s41598-018-19819-8 (2018).

3 Siegel, R. L., Miller, K. D. & Jemal, A. Cancer statistics, 2016. *CA Cancer J Clin* **66**, 7-30, doi:10.3322/caac.21332 (2016).

4 Society, C. C. Canadian Cancer Statistics 2019. (2019).

5 Sitarz, R. *et al*. Gastric cancer: epidemiology, prevention, classification, and treatment. *Cancer Manag Res* **10**, 239-248, doi:10.2147/CMAR.S149619 (2018).

6 Massarrat, S. & Stolte, M. Development of gastric cancer and its prevention. *Arch Iran Med* **17**, 514-520, doi:0141707/aim.0013 (2014).

7 Buckland, G. *et al*. Healthy lifestyle index and risk of gastric adenocarcinoma in the EPIC cohort study. *Int J Cancer* **137**, 598-606, doi:10.1002/ijc.29411 (2015).

8 Sakr, R., Massoud, M., Aftimos, G. & Chahine, G. Gastric Adenocarcinoma Secondary to Primary Gastric Diffuse Large B-cell Lymphoma. *J Gastric Cancer* **17**, 180-185, doi:10.5230/jgc.2017.17.e11 (2017).

9 Buas, M. F. & Vaughan, T. L. Epidemiology and risk factors for gastroesophageal junction tumors: understanding the rising incidence of this disease. *Semin Radiat Oncol* **23**, 3-9, doi:10.1016/j.semradonc.2012.09.008 (2013).

10 Ma, J., Shen, H., Kapesa, L. & Zeng, S. Lauren classification and individualized chemotherapy in gastric cancer. *Oncol Lett* **11**, 2959-2964, doi:10.3892/ol.2016.4337 (2016).

11 Hu, B. *et al*. Gastric cancer: Classification, histology and application of molecular pathology. *J Gastrointest Oncol* **3**, 251-261, doi:10.3978/j.issn.2078-6891.2012.021 (2012).

12 Ansari, S., Gantuya, B., Tuan, V. P. & Yamaoka, Y. Diffuse Gastric Cancer: A Summary of Analogous Contributing Factors for Its Molecular Pathogenicity. *Int J Mol Sci* **19**, doi:10.3390/ijms19082424 (2018).

13 Jain, S. & Dhingra, S. Pathology of esophageal cancer and Barrett's esophagus. *Ann Cardiothorac Surg* **6**, 99-109, doi:10.21037/acs.2017.03.06 (2017).

14 Zhang, Y. Epidemiology of esophageal cancer. *World J Gastroenterol* **19**, 5598-5606, doi:10.3748/wjg.v19.i34.5598 (2013).

15 Modiano, N. & Gerson, L. B. Barrett's esophagus: Incidence, etiology, pathophysiology, prevention and treatment. *Ther Clin Risk Manag* **3**, 1035-1145 (2007).

16 Liu, Y. *et al*. Comparative Molecular Analysis of Gastrointestinal Adenocarcinomas. *Cancer Cell* **33**, 721-735.e728, doi:10.1016/j.ccell.2018.03.010 (2018).

17 Ferri, L. E. *et al*. Perioperative docetaxel, cisplatin, and 5-fluorouracil (DCF) for locally advanced esophageal and gastric adenocarcinoma: a multicenter phase II trial. *Ann Oncol* **23**, 1512-1517, doi:10.1093/annonc/mdr465 (2012).

18 Ychou, M. *et al*. Perioperative chemotherapy compared with surgery alone for resectable gastroesophageal adenocarcinoma: an FNCLCC and FFCD multicenter phase III trial. *J Clin Oncol* **29**, 1715-1721, doi:10.1200/jco.2010.33.0597 (2011).

19 Cunningham, D. *et al*. Perioperative chemotherapy versus surgery alone for resectable gastroesophageal cancer. *N Engl J Med* **355**, 11-20, doi:10.1056/NEJMoa055531 (2006).
20 van Hagen, P. *et al*. Preoperative chemoradiotherapy for esophageal or junctional cancer. *N Engl J Med* **366**, 2074-2084, doi:10.1056/NEJMoa1112088 (2012).
21 Stahl, M. *et al*. Preoperative chemotherapy versus chemoradiotherapy in locally advanced adenocarcinomas of the oesophagogastric junction (POET): Long-term results of a controlled randomised trial. *Eur J Cancer* **81**, 183-190, doi:10.1016/j.ejca.2017.04.027 (2017).
22 Sudarshan, M. *et al*. Survival and recurrence patterns after neoadjuvant docetaxel, cisplatin, and 5-fluorouracil (DCF) for locally advanced esophagogastric adenocarcinoma. *Ann Surg Oncol* **22**, 324-330, doi:10.1245/s10434-014-3875-3 (2015).
23 Kang, Y. K. *et al*. Nivolumab in patients with advanced gastric or gastro-oesophageal junction cancer refractory to, or intolerant of, at least two previous chemotherapy regimens (ONO-4538-12, ATTRACTION-2): a randomised, double-blind, placebo-controlled, phase 3 trial. *Lancet* **390**, 2461-2471, doi:10.1016/s0140-6736(17)31827-5 (2017).
24 Moehler, M. H. *et al*. CheckMate 649: A randomized, multicenter, open-label, phase III study of nivolumab (NIVO) + ipilimumab (IPI) or nivo + chemotherapy (CTX) versus CTX alone in patients with previously untreated advanced (Adv) gastric (G) or gastroesophageal junction (GEJ) cancer. *Journal of Clinical Oncology* **36**, TPS192-TPS192, doi:10.1200/JCO.2018.36.4_suppl.TPS192 (2018).
25 Shitara, K. *et al*. Pembrolizumab versus paclitaxel for previously treated, advanced gastric or gastro-oesophageal junction cancer (KEYNOTE-061): a randomised, open-label, controlled, phase 3 trial. *Lancet* **392**, 123-133, doi:10.1016/s0140-6736(18)31257-1 (2018).
26 Bang, Y. J. *et al*. Efficacy of Sequential Ipilimumab Monotherapy versus Best Supportive Care for Unresectable Locally Advanced/Metastatic Gastric or Gastroesophageal Junction Cancer. *Clin Cancer Res* **23**, 5671-5678, doi:10.1158/1078-0432.Ccr-17-0025 (2017).
27 Comprehensive molecular characterization of gastric adenocarcinoma. *Nature* **513**, 202-209, doi:10.1038/nature13480 (2014).
28 Integrated genomic characterization of oesophageal carcinoma. *Nature* **541**, 169-175, doi:10.1038/nature20805 (2017).
29 Agrawal, N. *et al*. Comparative genomic analysis of esophageal adenocarcinoma and squamous cell carcinoma. *Cancer Discov* **2**, 899-905, doi:10.1158/2159-8290.CD-12-0189 (2012).
30 Abrahao-Machado, L. F. & Scapulatempo-Neto, C. HER2 testing in gastric cancer: An update. *World J Gastroenterol* **22**, 4619-4625, doi:10.3748/wjg.v22.i19.4619 (2016).
31 Bang, Y. J. *et al*. Trastuzumab in combination with chemotherapy versus chemotherapy alone for treatment of HER2-positive advanced gastric or gastro-oesophageal junction cancer (ToGA): a phase 3, open-label, randomised controlled trial. *Lancet* **376**, 687-697, doi:10.1016/s0140-6736(10)61121-x (2010).
32 Satoh, T. *et al*. Lapatinib plus paclitaxel versus paclitaxel alone in the second-line treatment of HER2-amplified advanced gastric cancer in Asian populations: TyTAN--a randomized, phase III study. *J Clin Oncol* **32**, 2039-2049, doi:10.1200/jco.2013.53.6136 (2014).

33 Kang, Y. K. *et al*. A phase IIa dose-finding and safety study of first-line pertuzumab in combination with trastuzumab, capecitabine and cisplatin in patients with HER2-positive advanced gastric cancer. *Br J Cancer* **111**, 660-666, doi:10.1038/bjc.2014.356 (2014).

34 Van Cutsem, E. *et al*. A randomized, open-label study of the efficacy and safety of AZD4547 monotherapy versus paclitaxel for the treatment of advanced gastric adenocarcinoma with FGFR2 polysomy or gene amplification. *Ann Oncol* **28**, 1316-1324, doi:10.1093/annonc/mdx107 (2017).

35 Catenacci, D. V. T. *et al*. Rilotumumab plus epirubicin, cisplatin, and capecitabine as first-line therapy in advanced MET-positive gastric or gastro-oesophageal junction cancer (RILOMET-1): a randomised, double-blind, placebo-controlled, phase 3 trial. *Lancet Oncol* **18**, 1467-1482, doi:10.1016/s1470-2045(17)30566-1 (2017).

36 Pectasides, E. *et al*. Genomic Heterogeneity as a Barrier to Precision Medicine in Gastroesophageal Adenocarcinoma. *Cancer Discov* **8**, 37-48, doi:10.1158/2159-8290.Cd-17-0395 (2018).

37 Kurokawa, Y. *et al*. Multicenter large-scale study of prognostic impact of HER2 expression in patients with resectable gastric cancer. *Gastric Cancer* **18**, 691-697, doi:10.1007/s10120-014-0430-7 (2015).

38 Gravalos, C. & Jimeno, A. HER2 in gastric cancer: a new prognostic factor and a novel therapeutic target. *Annals of Oncology* **19**, 1523-1529, doi:10.1093/annonc/mdn169 (2008).

39 Lote, H., Valeri, N. & Chau, I. HER2 inhibition in gastro-oesophageal cancer: A review drawing on lessons learned from breast cancer. *World J Gastrointest Oncol* **10**, 159-171, doi:10.4251/wjgo.v10.i7.159 (2018).

40 Hecht, J. R. *et al*. Lapatinib in Combination With Capecitabine Plus Oxaliplatin in Human Epidermal Growth Factor Receptor 2-Positive Advanced or Metastatic Gastric, Esophageal, or Gastroesophageal Adenocarcinoma: TRIO-013/LOGiC--A Randomized Phase III Trial. *J Clin Oncol* **34**, 443-451, doi:10.1200/jco.2015.62.6598 (2016).

41 Geyer, C. E. *et al*. Lapatinib plus Capecitabine for HER2-Positive Advanced Breast Cancer. *New England Journal of Medicine* **355**, 2733-2743, doi:10.1056/NEJMoa064320 (2006).

42 Baselga, J. *et al*. Pertuzumab plus trastuzumab plus docetaxel for metastatic breast cancer. *N Engl J Med* **366**, 109-119, doi:10.1056/NEJMoa1113216 (2012).

43 Tabernero, J. *et al*. Pertuzumab plus trastuzumab and chemotherapy for HER2-positive metastatic gastric or gastro-oesophageal junction cancer (JACOB): final analysis of a double-blind, randomised, placebo-controlled phase 3 study. *Lancet Oncol* **19**, 1372-1384, doi:10.1016/s1470-2045(18)30481-9 (2018).

44 Fuchs, C. S. *et al*. Biomarker analyses in REGARD gastric/GEJ carcinoma patients treated with VEGFR2-targeted antibody ramucirumab. *British journal of cancer* **115**, 974-982, doi:10.1038/bjc.2016.293 (2016).

45 Yang, W., Raufi, A. & Klempner, S. J. Targeted therapy for gastric cancer: molecular pathways and ongoing investigations. *Biochim Biophys Acta* **1846**, 232-237, doi:10.1016/j.bbcan.2014.05.003 (2014).

46 Juttner, S. *et al*. Vascular endothelial growth factor-D and its receptor VEGFR-3: two novel independent prognostic markers in gastric adenocarcinoma. *J Clin Oncol* **24**, 228-240, doi:10.1200/jco.2004.00.3467 (2006).

47 Ozdemir, F. *et al*. The effects of VEGF and VEGFR-2 on survival in patients with gastric cancer. *J Exp Clin Cancer Res* **25**, 83-88 (2006).
48 Fuchs, C. S. *et al*. Ramucirumab monotherapy for previously treated advanced gastric or gastro-oesophageal junction adenocarcinoma (REGARD): an international, randomised, multicentre, placebo-controlled, phase 3 trial. *Lancet* **383**, 31-39, doi:10.1016/s0140-6736(13)61719-5 (2014).
49 Wilke, H. *et al*. Ramucirumab plus paclitaxel versus placebo plus paclitaxel in patients with previously treated advanced gastric or gastro-oesophageal junction adenocarcinoma (RAINBOW): a double-blind, randomised phase 3 trial. *Lancet Oncol* **15**, 1224-1235, doi:10.1016/s1470-2045(14)70420-6 (2014).
50 Li, K. & Li, J. Current Molecular Targeted Therapy in Advanced Gastric Cancer: A Comprehensive Review of Therapeutic Mechanism, Clinical Trials, and Practical Application. *Gastroenterol Res Pract* **2016**, 4105615, doi:10.1155/2016/4105615 (2016).
51 Makiyama, A. *et al*. A randomized phase II study of weekly paclitaxel ± trastuzumab in patients with HER2-positive advanced gastric or gastro-esophageal junction cancer refractory to trastuzumab combined with fluoropyrimidine and platinum: WJOG7112G (T-ACT). *Journal of Clinical Oncology* **36**, 4011-4011, doi:10.1200/JCO.2018.36.15_suppl.4011 (2018).
52 De Vita, F. *et al*. Ramucirumab and paclitaxel in patients with gastric cancer and prior trastuzumab: subgroup analysis from RAINBOW study. *Future Oncol* **15**, 2723-2731, doi:10.2217/fon-2019-0243 (2019).
53 Ohtsu, A. *et al*. Bevacizumab in combination with chemotherapy as first-line therapy in advanced gastric cancer: a randomized, double-blind, placebo-controlled phase III study. *J Clin Oncol* **29**, 3968-3976, doi:10.1200/jco.2011.36.2236 (2011).
54 Chen, L.-T. *et al*. Anti-angiogenic Therapy in Patients with Advanced Gastric and Gastroesophageal Junction Cancer: A Systematic Review. *Cancer Res Treat* **49**, 851-868, doi:10.4143/crt.2016.176 (2017).
55 Li, J. *et al*. Randomized, Double-Blind, Placebo-Controlled Phase III Trial of Apatinib in Patients With Chemotherapy-Refractory Advanced or Metastatic Adenocarcinoma of the Stomach or Gastroesophageal Junction. *J Clin Oncol* **34**, 1448-1454, doi:10.1200/jco.2015.63.5995 (2016).
56 Tomas, A., Futter, C. E. & Eden, E. R. EGF receptor trafficking: consequences for signaling and cancer. *Trends Cell Biol* **24**, 26-34, doi:10.1016/j.tcb.2013.11.002 (2014).
57 NIH. Genomic Data Commons Data Portal. *The Cancer Genome Atlas* (2019).
58 Kim, M. A. *et al*. EGFR in gastric carcinomas: prognostic significance of protein overexpression and high gene copy number. *Histopathology* **52**, 738-746, doi:10.1111/j.1365-2559.2008.03021.x (2008).
59 Wang, D. *et al*. High expression of EGFR predicts poor survival in patients with resected T3 stage gastric adenocarcinoma and promotes cancer cell survival. *Oncol Lett* **13**, 3003-3013, doi:10.3892/ol.2017.5827 (2017).
60 Lordick, F. *et al*. Capecitabine and cisplatin with or without cetuximab for patients with previously untreated advanced gastric cancer (EXPAND): a randomised, open-label phase 3 trial. *The Lancet Oncology* **14**, 490-499, doi:https://doi.org/10.1016/S1470-2045(13)70102-5 (2013).
61 Okines, A. F. C. *et al*. Epirubicin, Oxaliplatin, and Capecitabine With or Without Panitumumab for Advanced Esophagogastric Cancer: Dose-Finding Study for the

Prospective Multicenter, Randomized, Phase II/III REAL-3 Trial. *Journal of Clinical Oncology* **28**, 3945-3950, doi:10.1200/JCO.2010.29.2847 (2010).

62 Dutton, S. J. *et al*. Gefitinib for oesophageal cancer progressing after chemotherapy (COG): a phase 3, multicentre, double-blind, placebo-controlled randomised trial. *Lancet Oncol* **15**, 894-904, doi:10.1016/s1470-2045(14)70024-5 (2014).

63 Maron, S. B. *et al*. Targeted Therapies for Targeted Populations: Anti-EGFR Treatment for <em>EGFR</em>-Amplified Gastroesophageal Adenocarcinoma. *Cancer Discov* **8**, 696, doi:10.1158/2159-8290.CD-17-1260 (2018).

64 Petty, R., Dahle-Smith, A., Stevenson, D., Dutton, S. & Roberts, C. Gefitinib and Epidermal Growth Factor Receptor Gene Copy Number Aberrations in Esophageal Cancer. *Journal of Clinical Oncology* **35**, 2279-2287 (2017).

65 Luber, B. *et al*. Biomarker analysis of cetuximab plus oxaliplatin/leucovorin/5-fluorouracil in first-line metastatic gastric and oesophago-gastric junction cancer: results from a phase II trial of the Arbeitsgemeinschaft Internistische Onkologie (AIO). *BMC Cancer* **11**, 509, doi:10.1186/1471-2407-11-509 (2011).

66 Lordick, F. *et al*. Clinical outcome according to tumor HER2 status and EGFR expression in advanced gastric cancer patients from the EXPAND study. *Journal of Clinical Oncology* **31**, 4021-4021, doi:10.1200/jco.2013.31.15_suppl.4021 (2013).

67 Katoh, M. & Katoh, M. FGF signaling network in the gastrointestinal tract (review). *Int J Oncol* **29**, 163-168 (2006).

68 Deng, N. *et al*. A comprehensive survey of genomic alterations in gastric cancer reveals systematic patterns of molecular exclusivity and co-occurrence among distinct therapeutic targets. *Gut* **61**, 673, doi:10.1136/gutjnl-2011-301839 (2012).

69 Su, X. *et al*. FGFR2 amplification has prognostic significance in gastric cancer: results from a large international multicentre study. *British Journal Of Cancer* **110**, 967, doi:10.1038/bjc.2013.802 (2014).

70 Kim, H. S., Kim, J. H., Jang, H. J., Han, B. & Zang, D. Y. Pathological and Prognostic Impacts of FGFR2 Overexpression in Gastric Cancer: A Meta-Analysis. *J Cancer* **10**, 20-27, doi:10.7150/jca.28204 (2019).

71 Xie, L. *et al*. <em>FGFR2</em> Gene Amplification in Gastric Cancer Predicts Sensitivity to the Selective FGFR Inhibitor AZD4547. *Clinical Cancer Research* **19**, 2572, doi:10.1158/1078-0432.CCR-12-3898 (2013).

72 Yashiro, M. & Matsuoka, T. Fibroblast growth factor receptor signaling as therapeutic targets in gastric cancer. *World J Gastroenterol* **22**, 2415-2423, doi:10.3748/wjg.v22.i8.2415 (2016).

73 Birchmeier, C., Birchmeier, W., Gherardi, E. & Vande Woude, G. F. Met, metastasis, motility and more. *Nature Reviews Molecular Cell Biology* **4**, 915-925, doi:10.1038/nrm1261 (2003).

74 Graziano, F. *et al*. Genetic Activation of the MET Pathway and Prognosis of Patients With High-Risk, Radically Resected Gastric Cancer. *Journal of Clinical Oncology* **29**, 4789-4795, doi:10.1200/JCO.2011.36.7706 (2011).

75 Lee, H. E. *et al*. MET in gastric carcinomas: comparison between protein expression and gene copy number and impact on clinical outcome. *Br J Cancer* **107**, 325-333, doi:10.1038/bjc.2012.237 (2012).

76 Shah, M. A. *et al*. METGastric: A phase III study of onartuzumab plus mFOLFOX6 in patients with metastatic HER2-negative (HER2-) and MET-positive (MET+)

adenocarcinoma of the stomach or gastroesophageal junction (GEC). *Journal of Clinical Oncology* **33**, 4012-4012, doi:10.1200/jco.2015.33.15_suppl.4012 (2015).

77 Kataoka, Y. *et al*. Foretinib (GSK1363089), a multi-kinase inhibitor of MET and VEGFRs, inhibits growth of gastric cancer cell lines by blocking inter-receptor tyrosine kinase networks. *Invest New Drugs* **30**, 1352-1360, doi:10.1007/s10637-011-9699-0 (2012).

78 Shah, M. A. *et al*. Phase II study evaluating 2 dosing schedules of oral foretinib (GSK1363089), cMET/VEGFR2 inhibitor, in patients with metastatic gastric cancer. *PLoS One* **8**, e54014, doi:10.1371/journal.pone.0054014 (2013).

79 Plotnikov, A., Zehorai, E., Procaccia, S. & Seger, R. The MAPK cascades: signaling components, nuclear roles and mechanisms of nuclear translocation. *Biochim Biophys Acta* **1813**, 1619-1633, doi:10.1016/j.bbamcr.2010.12.012 (2011).

80 Marampon, F., Ciccarelli, C. & Zani, B. M. Biological Rationale for Targeting MEK/ERK Pathways in Anti-Cancer Therapy and to Potentiate Tumour Responses to Radiation. *Int J Mol Sci* **20**, doi:10.3390/ijms20102530 (2019).

81 Lee, S. H. *et al*. BRAF and KRAS mutations in stomach cancer. *Oncogene* **22**, 6942-6945, doi:10.1038/sj.onc.1206749 (2003).

82 Hewitt, L. C., Hutchins, G. G., Melotte, V., Saito, Y. & Grabsch, H. I. KRAS, BRAF and gastric cancer. *Translational Gastrointestinal Cancer* **4**, 429-447 (2015).

83 Chapman, P. B. *et al*. Improved Survival with Vemurafenib in Melanoma with BRAF V600E Mutation. *New England Journal of Medicine* **364**, 2507-2516, doi:10.1056/NEJMoa1103782 (2011).

84 Hauschild, A. *et al*. Dabrafenib in BRAF-mutated metastatic melanoma: a multicentre, open-label, phase 3 randomised controlled trial. *The Lancet* **380**, 358-365, doi:https://doi.org/10.1016/S0140-6736(12)60868-X (2012).

85 Robert, C. *et al*. Five-Year Outcomes with Dabrafenib plus Trametinib in Metastatic Melanoma. *N Engl J Med* **381**, 626-636, doi:10.1056/NEJMoa1904059 (2019).

86 Queirolo, P., Picasso, V. & Spagnolo, F. Combined BRAF and MEK inhibition for the treatment of BRAF-mutated metastatic melanoma. *Cancer Treatment Reviews* **41**, 519-526, doi:https://doi.org/10.1016/j.ctrv.2015.04.010 (2015).

87 Sullivan, R. J. *et al*. First-in-Class ERK1/2 Inhibitor Ulixertinib (BVD-523) in Patients with MAPK Mutant Advanced Solid Tumors: Results of a Phase I Dose-Escalation and Expansion Study. *Cancer Discov* **8**, 184-195, doi:10.1158/2159-8290.Cd-17-1119 (2018).

88 Mizukami, T. *et al*. EGFR and HER2 signals play a salvage role in MEK1-mutated gastric cancer after MEK inhibition. *Int J Oncol* **47**, 499-505, doi:10.3892/ijo.2015.3050 (2015).

89 Wong, G. S. *et al*. Targeting wild-type KRAS-amplified gastroesophageal cancer through combined MEK and SHP2 inhibition. *Nat Med* **24**, 968-977, doi:10.1038/s41591-018-0022-x (2018).

90 Tran, P., Nguyen, C. & Klempner, S. J. Targeting the Phosphatidylinositol-3-kinase Pathway in Gastric Cancer: Can Omics Improve Outcomes? *Int Neurourol J* **20**, S131-S140, doi:10.5213/inj.1632740.370 (2016).

91 Janku, F., Yap, T. A. & Meric-Bernstam, F. Targeting the PI3K pathway in cancer: are we making headway? *Nature Reviews Clinical Oncology* **15**, 273, doi:10.1038/nrclinonc.2018.28 (2018).

92 Klempner, S. J., Myers, A. P. & Cantley, L. C. What a tangled web we weave: emerging resistance mechanisms to inhibition of the phosphoinositide 3-kinase pathway. *Cancer Discov* **3**, 1345-1354, doi:10.1158/2159-8290.Cd-13-0063 (2013).

93 Markman, B., Atzori, F., Perez-Garcia, J., Tabernero, J. & Baselga, J. Status of PI3K inhibition and biomarker development in cancer therapeutics. *Ann Oncol* **21**, 683-691, doi:10.1093/annonc/mdp347 (2010).

94 Shi, J. *et al*. Highly frequent PIK3CA amplification is associated with poor prognosis in gastric cancer. *BMC cancer* **12**, 50-50, doi:10.1186/1471-2407-12-50 (2012).

95 Nam, S. Y. *et al*. Akt/PKB activation in gastric carcinomas correlates with clinicopathologic variables and prognosis. *Apmis* **111**, 1105-1113, doi:10.1111/j.1600-0463.2003.apm1111205.x (2003).

96 Ohtsu, A. *et al*. Everolimus for previously treated advanced gastric cancer: results of the randomized, double-blind, phase III GRANITE-1 study. *J Clin Oncol* **31**, 3935-3943, doi:10.1200/jco.2012.48.3552 (2013).

97 Ramanathan, R. K. *et al*. Phase 2 study of MK-2206, an allosteric inhibitor of AKT, as second-line therapy for advanced gastric and gastroesophageal junction cancer: A SWOG cooperative group trial (S1005). *Cancer* **121**, 2193-2197, doi:10.1002/cncr.29363 (2015).

98 Chen, D. *et al*. Dual PI3K/mTOR inhibitor BEZ235 as a promising therapeutic strategy against paclitaxel-resistant gastric cancer via targeting PI3K/Akt/mTOR pathway. *Cell Death Dis* **9**, 123, doi:10.1038/s41419-017-0132-2 (2018).

99 Shen, J. *et al*. ARID1A Deficiency Impairs the DNA Damage Checkpoint and Sensitizes Cells to PARP Inhibitors. *Cancer Discov* **5**, 752, doi:10.1158/2159-8290.CD-14-0849 (2015).

100 Chandler, R. L. *et al*. ARID1a-DNA interactions are required for promoter occupancy by SWI/SNF. *Mol Cell Biol* **33**, 265-280, doi:10.1128/mcb.01008-12 (2013).

101 Wu, R.-C., Wang, T.-L. & Shih, I.-M. The emerging roles of ARID1A in tumor suppression. *Cancer Biol Ther* **15**, 655-664, doi:10.4161/cbt.28411 (2014).

102 Inada, R. *et al*. ARID1A expression in gastric adenocarcinoma: clinicopathological significance and correlation with DNA mismatch repair status. *World J Gastroenterol* **21**, 2159-2168, doi:10.3748/wjg.v21.i7.2159 (2015).

103 Zhou, H., Tan, S., Li, H. & Lin, X. Expression and significance of EBV, ARID1A and PIK3CA in gastric carcinoma. *Mol Med Rep* **19**, 2125-2136, doi:10.3892/mmr.2019.9886 (2019).

104 Chandler, R. L. *et al*. Coexistent ARID1A-PIK3CA mutations promote ovarian clear-cell tumorigenesis through pro-tumorigenic inflammatory cytokine signalling. *Nat Commun* **6**, 6118-6118, doi:10.1038/ncomms7118 (2015).

105 Caumanns, J. J., Wisman, G. B. A., Berns, K., van der Zee, A. G. J. & de Jong, S. ARID1A mutant ovarian clear cell carcinoma: A clear target for synthetic lethal strategies. *Biochimica et Biophysica Acta (BBA) - Reviews on Cancer* **1870**, 176-184, doi:https://doi.org/10.1016/j.bbcan.2018.07.005 (2018).

106 Williamson, C. T. *et al*. ATR inhibitors as a synthetic lethal therapy for tumours deficient in ARID1A. *Nat Commun* **7**, 13837, doi:10.1038/ncomms13837 (2016).

107 Lee, D., Yu, E. J., Ham, I.-H., Hur, H. & Kim, Y.-S. AKT inhibition is an effective treatment strategy in ARID1A-deficient gastric cancer cells. *Onco Targets Ther* **10**, 4153-4159, doi:10.2147/OTT.S139664 (2017).

108 Yin, N. *et al*. Synergistic and antagonistic drug combinations depend on network topology. *PloS one* **9**, e93960-e93960, doi:10.1371/journal.pone.0093960 (2014).

109 Engelman, J. A. *et al*. Effective use of PI3K and MEK inhibitors to treat mutant Kras G12D and PIK3CA H1047R murine lung cancers. *Nat Med* **14**, 1351-1356, doi:10.1038/nm.1890 (2008).

110 Belmont, P. J. *et al*. Resistance to dual blockade of the kinases PI3K and mTOR in KRAS-mutant colorectal cancer models results in combined sensitivity to inhibition of the receptor tyrosine kinase EGFR. *Sci Signal* **7**, ra107, doi:10.1126/scisignal.2005516 (2014).

111 Sheppard, K. E. *et al*. Synergistic inhibition of ovarian cancer cell growth by combining selective PI3K/mTOR and RAS/ERK pathway inhibitors. *Eur J Cancer* **49**, 3936-3944, doi:10.1016/j.ejca.2013.08.007 (2013).

112 Prasad, V. & Mailankody, S. Research and Development Spending to Bring a Single Cancer Drug to Market and Revenues After Approval. *JAMA Intern Med* **177**, 1569-1575, doi:10.1001/jamainternmed.2017.3601 (2017).

113 Lin, M., Gao, M., Cavnar, M. J. & Kim, J. Utilizing gastric cancer organoids to assess tumor biology and personalize medicine. *World J Gastrointest Oncol* **11**, 509-517, doi:10.4251/wjgo.v11.i7.509 (2019).

114 Hughes, C. S., Postovit, L. M. & Lajoie, G. A. Matrigel: A complex protein mixture required for optimal growth of cell culture. *PROTEOMICS* **10**, 1886-1890, doi:10.1002/pmic.200900758 (2010).

115 Barker, N. *et al*. Lgr5+ve Stem Cells Drive Self-Renewal in the Stomach and Build Long-Lived Gastric Units In Vitro. *Cell Stem Cell* **6**, 25-36, doi:https://doi.org/10.1016/j.stem.2009.11.013 (2010).

116 Frattini, A. *et al*. High variability of genomic instability and gene expression profiling in different HeLa clones. *Scientific Reports* **5**, 15377, doi:10.1038/srep15377 (2015).

117 Gao, M. *et al*. Development of Patient-Derived Gastric Cancer Organoids from Endoscopic Biopsies and Surgical Tissues. *Annals of Surgical Oncology* **25**, 2767-2775, doi:10.1245/s10434-018-6662-8 (2018).

118 Bartfeld, S. & Clevers, H. Stem cell-derived organoids and their application for medical research and patient treatment. *Journal of Molecular Medicine* **95**, 729-738, doi:10.1007/s00109-017-1531-7 (2017).

119 Hidalgo, M. *et al*. Patient-Derived Xenograft Models: An Emerging Platform for Translational Cancer Research. *Cancer Discov* **4**, 998, doi:10.1158/2159-8290.CD-14-0001 (2014).

120 Tuveson, D. & Clevers, H. Cancer modeling meets human organoid technology. *Science* **364**, 952, doi:10.1126/science.aaw6985 (2019).

121 Boj, S. F. *et al*. Organoid models of human and mouse ductal pancreatic cancer. *Cell* **160**, 324-338, doi:10.1016/j.cell.2014.12.021 (2015).

122 Yan, H. H. N. *et al*. A Comprehensive Human Gastric Cancer Organoid Biobank Captures Tumor Subtype Heterogeneity and Enables Therapeutic Screening. *Cell Stem Cell* **23**, 882-897.e811, doi:https://doi.org/10.1016/j.stem.2018.09.016 (2018).

123 Weeber, F. *et al*. Preserved genetic diversity in organoids cultured from biopsies of human colorectal cancer metastases. *Proceedings of the National Academy of Sciences* **112**, 13308, doi:10.1073/pnas.1516689112 (2015).

124 Drost, J. *et al*. Sequential cancer mutations in cultured human intestinal stem cells. *Nature* **521**, 43-47, doi:10.1038/nature14415 (2015).
125 Vlachogiannis, G. *et al*. Patient-derived organoids model treatment response of metastatic gastrointestinal cancers. *Science* **359**, 920, doi:10.1126/science.aao2774 (2018).
126 Tiriac, H. *et al*. Organoid Profiling Identifies Common Responders to Chemotherapy in Pancreatic Cancer. *Cancer Discov* **8**, 1112-1129, doi:10.1158/2159-8290.Cd-18-0349 (2018).
127 Medina, P. J. & Goodin, S. Lapatinib: A dual inhibitor of human epidermal growth factor receptor tyrosine kinases. *Clinical Therapeutics* **30**, 1426-1447, doi:https://doi.org/10.1016/j.clinthera.2008.08.008 (2008).
128 Fujii, M., Clevers, H. & Sato, T. Modeling Human Digestive Diseases With CRISPR-Cas9–Modified Organoids. *Gastroenterology* **156**, 562-576, doi:10.1053/j.gastro.2018.11.048 (2019).
129 Yoshida, G. J. Applications of patient-derived tumor xenograft models and tumor organoids. *Journal of Hematology & Oncology* **13**, 4, doi:10.1186/s13045-019-0829-z (2020).
130 Fernández, M. L. *et al*. Differences in MEK inhibitor efficacy in molecularly characterized low-grade serous ovarian cancer cell lines. *Am J Cancer Res* **6**, 2235-2251 (2016).
131 Ward, R. A. *et al*. Structure-Guided Design of Highly Selective and Potent Covalent Inhibitors of ERK1/2. *J Med Chem* **58**, 4790-4801, doi:10.1021/acs.jmedchem.5b00466 (2015).
132 Carter, A. J. & Nguyen, C. N. A comparison of cancer burden and research spending reveals discrepancies in the distribution of research funding. *BMC Public Health* **12**, 526, doi:10.1186/1471-2458-12-526 (2012).
133 Mizrak Kaya, D., Harada, K. & Ajani, J. A. Is targeted therapy possible for patients with gastric adenocarcinoma? *Expert Opin Pharmacother* **17**, 2371-2374, doi:10.1080/14656566.2016.1236917 (2016).
134 Verret, B., Cortes, J., Bachelot, T., Andre, F. & Arnedos, M. Efficacy of PI3K inhibitors in advanced breast cancer. *Annals of oncology : official journal of the European Society for Medical Oncology* **30**, x12-x20, doi:10.1093/annonc/mdz381 (2019).
135 Kelly, R. J. Dabrafenib and trametinib for the treatment of non-small cell lung cancer. *Expert Rev Anticancer Ther* **18**, 1063-1068, doi:10.1080/14737140.2018.1521272 (2018).
136 Kwan, S.-Y. *et al*. Loss of ARID1A expression leads to sensitivity to ROS-inducing agent elesclomol in gynecologic cancer cells. *Oncotarget; Vol 7, No 35* (2016).
137 Samartzis, E. P. *et al*. Loss of ARID1A expression sensitizes cancer cells to PI3K- and AKT-inhibition. *Oncotarget; Vol 5, No 14* (2014).
138 Bitler, B. G. *et al*. Synthetic lethality by targeting EZH2 methyltransferase activity in ARID1A-mutated cancers. *Nat Med* **21**, 231-238, doi:10.1038/nm.3799 (2015).
139 Berns, K. *et al*. Loss of <em>ARID1A</em> Activates <em>ANXA1</em>, which Serves as a Predictive Biomarker for Trastuzumab Resistance. *Clinical Cancer Research* **22**, 5238, doi:10.1158/1078-0432.CCR-15-2996 (2016).

140 Gilmartin, A. G. *et al*. GSK1120212 (JTP-74057) is an inhibitor of MEK activity and activation with favorable pharmacokinetic properties for sustained in vivo pathway inhibition. *Clin Cancer Res* **17**, 989-1000, doi:10.1158/1078-0432.Ccr-10-2200 (2011).

141 Institute, N. C. *Clinical Trials Using Trametinib*, <https://www.cancer.gov/about-cancer/treatment/clinical-trials/intervention/trametinib> (2020).

142 Evangelisti, C. *et al*. Targeted inhibition of mTORC1 and mTORC2 by active-site mTOR inhibitors has cytotoxic effects in T-cell acute lymphoblastic leukemia. *Leukemia* **25**, 781-791, doi:10.1038/leu.2011.20 (2011).

143 Zhao, D., Jiang, M., Zhang, X. & Hou, H. The role of RICTOR amplification in targeted therapy and drug resistance. *Mol Med* **26**, 20-20, doi:10.1186/s10020-020-0146-6 (2020).

144 Wainberg, Z. A. *et al*. Phase I study of the PI3K/mTOR inhibitor gedatolisib (PF-05212384) in combination with docetaxel, cisplatin, and dacomitinib. *Journal of Clinical Oncology* **34**, 2566-2566, doi:10.1200/JCO.2016.34.15_suppl.2566 (2016).

145 Soares, H. P. *et al*. Dual PI3K/mTOR Inhibitors Induce Rapid Overactivation of the MEK/ERK Pathway in Human Pancreatic Cancer Cells through Suppression of mTORC2. *Mol Cancer Ther* **14**, 1014-1023, doi:10.1158/1535-7163.MCT-14-0669 (2015).